HHS Public Access

Author manuscript

Nat Metab. Author manuscript; available in PMC 2022 April 18.

Published in final edited form as:

Nat Metab. 2021 October ; 3(10): 1327–1341. doi:10.1038/s42255-021-00466-9.

Fasting drives the metabolic, molecular, and geroprotective effects of a calorie restricted diet in mice

Heidi H. Pak[1,2,3], **Spencer A. Haws**[3,4,5], **Cara L. Green**[1,2], **Mikaela Koller**[1,2], **Mitchell T. Lavarias**[3,6], **Nicole E. Richardson**[1,2,7], **Shany E. Yang**[1,2], **Sabrina N. Dumas**[1,2], **Michelle Sonsalla**[1,2], **Lindsey Bray**[1,2], **Michelle Johnson**[8], **Stephen Barnes**[9], **Victor Darley-Usmar**[8], **Jianhua Zhang**[8], **Chi-Liang Eric Yen**[3,6], **John M. Denu**[3,4,5], **Dudley W. Lamming**[1,2,3,7,10]

[1]Department of Medicine, University of Wisconsin-Madison, Madison, WI

[2]William S. Middleton Memorial Veterans Hospital, Madison, WI

[3]Interdisciplinary Graduate Program in Nutritional Sciences, University of Wisconsin-Madison, Madison, WI, USA

[4]Department of Biomolecular Chemistry, University of Wisconsin-Madison, Madison, WI

[5]Wisconsin Institute for Discovery, Madison, WI, USA

[6]Department of Nutritional Sciences, University of Wisconsin-Madison, Madison, WI

[7]Endocrinology and Reproductive Physiology Graduate Training Program, University of Wisconsin-Madison, Madison, WI, USA

[8]Nathan Shock Center of Excellence in the Basic Biology of Aging, Department of Pathology, University of Alabama Birmingham

[9]Department of Pharmacology, University of Alabama Birmingham

Abstract

Calorie restriction (CR) promotes healthy aging in diverse species. Recently, it has been shown that fasting for a portion of each day has metabolic benefits and promotes lifespan. These findings complicate the interpretation of rodent CR studies, in which animals typically eat only once per day and rapidly consume their food, which collaterally imposes fasting. Here, we show that a prolonged fast is necessary for key metabolic, molecular and geroprotective effects of a CR diet. Using a series of feeding regimens, we dissect the effects of calories and fasting, and proceed to

[10]**Correspondence and Lead Contact:** Dudley W. Lamming, PhD, Associate Professor of Medicine, University of Wisconsin-Madison, 2500 Overlook Terrace, VAH C3127 Research 151, Madison, WI 53705, USA, dlamming@medicine.wisc.edu, Tel: 608-256-1901 x12861, Fax: 608-263-9983;.

AUTHOR CONTRIBUTIONS

Experiments were performed in the Lamming, Denu, and Yen laboratories at UW-Madison and in the UAB Nathan Shock Center Mitometabolism Core. All authors participated in the performance of the experiments and/or analyzed the data. HHP, SAH, JZ, JMD and DWL prepared the manuscript.

COMPETING INTERESTS

D.W.L has received funding from, and is a scientific advisory board member of, Aeovian Pharmaceuticals, which seeks to develop novel, selective mTOR inhibitors for the treatment of various diseases. J.M.D. is a consultant for FORGE Life Sciences and co-founder of Galilei Bio-Sciences. The remaining authors declare no competing interests.

demonstrate that fasting alone recapitulates many of the physiological and molecular effects of CR. Our results shed new light on how both when and how much we eat regulate metabolic health and longevity, and demonstrate that daily prolonged fasting, and not solely reduced calorie intake, is likely responsible for the metabolic and geroprotective benefits of a CR diet.

Keywords

calorie restriction; fasting; dietary restriction; time-restricted feeding; lifespan; healthspan

Introduction

Calorie restriction (CR) is the gold standard for geroprotective interventions, extending lifespan and healthspan in diverse organisms and preventing or delaying many age-associated diseases[1–6]. In rodents, CR improves metabolic health and glucose homeostasis[1,7]. As long-term adherence to a reduced calorie diet is difficult for many people, there is significant interest in identifying the physiological and molecular mechanisms that mediate the beneficial effects of a CR diet.

Traditionally, the beneficial effects of a CR diet were believed to be the result of reduced caloric intake, although recent studies suggest that reduction of specific macronutrients may also play a role[8–14]. It has recently been realized that CR regimens, as typically implemented in the laboratory, not only restrict calories, but also impose a prolonged daily fast, as CR animals rapidly consume their entire daily meal within ~2 hours, and then fast for ~22 hours until their next meal[15–17]. Interventions such as time-restricted or meal feeding that involve a fasting period have metabolic benefits and extend the lifespan of mice[18–20]. These findings complicate the interpretation of CR studies, as it is unclear which effects of CR result from reduced caloric intake, and which instead are attributable to the collaterally imposed fast.

We developed a series of diets and feeding regimens enabling us to dissect the contribution of fasting from energy restriction alone in a CR diet. As different strains and sexes have differential responses to a CR diet[21,22], we examined the metabolic responses of both male and female C57BL/6J and DBA/2J mice. We also tested whether prolonged daily fasting without energy restriction could recapitulate the metabolic and transcriptional effects of a CR diet. Finally, we tested if fasting is required for the beneficial effects of a CR diet on healthspan and longevity.

We find that fasting is required for CR-induced changes in insulin sensitivity and fuel selection. Additionally, fasting alone without reduced energy intake is sufficient to recapitulate the metabolic phenotypes and transcriptional signature of a CR diet. Finally, we show that fasting is required for CR-induced improvements in glucose metabolism, frailty, and lifespan in C57BL/6J male mice. Our results overturn the long-held belief that the beneficial effects of a CR diet in mammals are mediated solely by the reduction of caloric intake, and highlight fasting as an important component of the metabolic and geroprotective effects of CR.

Results

The response of C57BL/6J males to multiple feeding paradigms

We acclimated 9-week old C57BL/6J male (B6M) mice for one week to a chow based diet (Envigo Global 2018)[21]. The animals were then weighed and randomized to one of four dietary regimens (Fig. 1A):

1. AL, mice given *ad libitum* access to a normal rodent diet (Envigo Global 2018, Supplementary Table 1);
2. Diluted AL, mice provided with *ad libitum* access to Envigo Global 2018 diluted 50% with indigestible cellulose (TD.170950, Supplementary Table 1); equivalent to 30% restriction of calories without imposed fasting[8];
3. MF.cr, mice were fed 30% less food than AL-fed mice, using an automatic feeder to release food in three equal portions during the 12-hour dark period; meal feeding (MF) reduces fasting period and binging behavior;
4. CR, mice fed once per day in the morning; with 30% restriction relative to the AL group and prolonged inter-meal fasting.

The time of feeding for the CR and MF.cr diets were carefully considered. Feeding CR mice once-per-day in the morning has been widely utilized for CR studies, including by the NIA Aging Rodent Colony[23]; and is well established to extend lifespan. Furthermore, the time-of-day at which the feeding of CR mice occurs does not affect the ability of CR to extend lifespan[24]. Feeding MF.cr mice overnight during the dark cycle aligns the completion-of-feeding time of the CR and MF.cr groups; and this MF.cr regimen is similar to a regimen previously shown to extend the lifespan of mice[24].

Some of the most well-established effects of a CR diet include reduced weight gain and adiposity[7,25,26]. Tracking the mice on each diet regimen, we found that all three dietary restriction regimens reduced weight gain, fat mass, and adiposity (Figs. 1B–E, Supplementary Table 2A). Despite all three diets reducing calorie intake by 30% (Extended Fig. 1A), there were clear differences between the effects of the diets. CR-fed mice gained more weight than mice fed the Diluted AL diet or the MF.cr diet (Fig. 1B, Supplementary Table 2A). Additionally, all three groups initially lost lean (fat-free) mass to differing degrees, although lean mass eventually rebounded in CR-fed mice (Fig. 1C, Supplementary Table 2B).

Fasting is required for CR-induced insulin sensitivity

Improved regulation of blood glucose is a conserved mammalian response to CR[1]. We examined the contribution of fasting and energy restriction on glucose homeostasis by performing glucose and insulin tolerance tests (Figs. 1F–G, Extended Figs. 1B–C), timing the assays such that mice in all groups were fasted for similar lengths of time. We found that all three restricted diets improved glucose tolerance after 9 weeks on diet (Fig. 1F) and similarly after 13 weeks on diet (Extended Fig. 1B). Surprisingly, we observed that insulin sensitivity as assessed by intraperitoneal (IP) insulin tolerance test was significantly improved only in mice fed the classic CR diet, and not in Diluted AL-fed or MF.cr-fed

mice (Fig. 1G, Extended Fig. 1C). Improved glucose tolerance was not due to increased insulin secretion, and calculated HOMA-IR did not differ significantly between groups (Extended Figs. 1D–F). These results suggest that fasting, and not a reduction in energy intake, mediates the improved insulin sensitivity of CR-fed animals.

Distinct fuel source utilization in CR is driven by fasting

CR-fed mice engage in rapid lipogenesis following refeeding, then sustain themselves via the utilization of these stored lipids[7,16]. We placed mice in metabolic chambers, allowing us to determine substrate utilization by examining the respiratory exchange ratio (RER). RER is calculated from the ratio of O_2 consumed and CO_2 produced; a value close to 1.0 indicates that carbohydrates are primarily utilized for energy production, while a value approaching 0.7 indicates that lipids are the predominant energy source[27]. An RER >1.0 reflects the utilization of carbohydrates for active *de novo* lipogenesis[16]. AL and Diluted AL-fed mice had *ad libitum* access to food while in the metabolic chambers; CR and MF.cr mice were fed at the same time at the beginning of the light cycle while in the chambers, as technical limitations made feeding the MF.cr mice multiple times during the dark cycle impractical. We observed that RER rapidly rose above 1.0 following refeeding, and then fell below 0.8 during the dark cycle, a fuel-source utilization pattern clearly distinct from that of AL-fed mice (Fig. 1H). Calculating fatty acid and carbohydrate/protein oxidation[16], we find that CR and MF.cr diets, but not the Diluted AL diet, increased fatty acid oxidation (Fig. 1I).

We examined the contribution of fasting and calories to energy expenditure (Supplementary Fig. 1A), correcting for differences in lean mass (Fig. 1J) and body weight (Supplementary Fig. 1B) using analysis of covariance (ANCOVA). As expected, mice consuming fewer calories had decreased energy expenditure relative to AL-fed mice; this effect was dependent on feeding regimen and not body weight. CR-fed and MF.cr-fed mice were more active immediately preceding and following feeding (Supplementary Figs. 1C–E); however, as activity accounts for only about 10% of mouse energy expenditure[28], the decreased energy intake of these mice is likely the primary factor in the reduced energy expenditure. These results suggest that fasting, and not a reduction in calories, is responsible for the altered fuel utilization of CR-fed animals, while the reduction in calories results in an overall decrease in exergy expenditure.

Fasting produces the distinct molecular signature of CR

We performed metabolomics on the livers of AL, CR, and Diluted AL-fed mice (Extended Fig. 2), targeting 59 metabolites in three broad groups based on their chemical structures – Amino Acids, Carbohydrates and Nucleoside/Nucleotides. We analyzed CR-fed mice under two feeding conditions. First, we collected tissues from CR mice that were fed 22 hours previously (CR-Fasted), while AL and Diluted AL groups were fed *ad libitum* overnight, and food was removed in the morning four hours prior to sacrifice, similar conditions as done in previous literature[21]. We also collected tissues from CR mice fed at the start of the light cycle for 3 hours prior to sacrifice (CR-Fed).

We identified 18 metabolites significantly altered in classical CR-Fasted mice as compared to compared to AL-fed mice; in contrast, we observed no differences between Diluted AL-

fed mice and AL-fed mice (Extended Fig. 2A, Supplementary Table 3). The metabolomic signature of CR-Fasted mice was distinct from both AL and Diluted AL-fed mice, while the latter two groups overlapped (Extended Fig. 2B). The metabolomic signatures of CR-Fed mice were metabolically distinct from AL-fed mice (Extended Figs. 2A, 2C), suggesting that CR-fed animals have distinct liver metabolomic signatures from AL-fed mice regardless of feeding state. Nucleotides/nucleosides and metabolites involved in carbohydrate metabolism were more significantly altered in fasted than fed state, with the exception of alpha-ketoglutarate (Extended Figs. 3A–B). We found broad changes in amino acid metabolism, with leucine, ornithine and proline significantly elevated in both CR-Fasted and CR-Fed groups relative to AL-fed controls (Extended Fig. 3C). Additionally, three amino acids – lysine, isoleucine and tryptophan – trended upwards in CR-Fasted mice and were significantly elevated in CR-Fed mice (Extended Fig. 3C).

Intriguingly, levels of methionine and S-adenosylhomocysteine (SAH), a metabolite of SAM consuming methyltransferase reactions, were elevated in the livers of CR mice (Extended Fig. 2D). Changes in levels of methionine and methionine metabolites can result in epigenetic changes, altering global histone post-translational modifications (PTM)[29,30]. We observed changes in global histone PTMs in the livers of both Diluted AL and CR-fed mice, with the CR diet resulting in a greater number of significantly altered histone PTMs (Extended Fig. 4, Supplementary Table 4). CR-fed mice possessed a distinct histone PTM profile compared to both AL-fed and Diluted AL-fed mice, which were more similar to each other (Extended Fig. 4A–B). Restriction of calories non-specifically increased H3 acetylation and non-specifically decreased H4 acetylation (Extended Fig. 4C). Tri-methylation of H3 Lys 27 (H3K27), a modification strongly associated with chromatin silencing[31], increased in CR-fed mice; di-methylation of H3K9 decreased while acetylation of H3K9/K14 increased. Our results suggest that prolonged fasting, not simply a reduction of calorie intake, is required for the epigenetic effects of a CR diet.

We also conducted targeted metabolomics in skeletal muscle[32–37] (Extended Fig. 5, Supplementary Table 5). We found many metabolites were altered in both CR-fed mice and Diluted-AL-fed mice as compared to AL-fed controls (Extended Fig. 5A). CR-fed mice had a distinct metabolomic signature from AL-fed mice; however, unlike in the liver, Diluted AL-fed mice had a distinct signature from AL-fed mice (Extended Fig. 5B). CR and Diluted AL-fed mice had similar changes in multiple TCA-cycle metabolites with the exception of Malate and 2-OHG. Although prolonged fasting is required to produce the distinct metabolomic signature of CR in both the liver and skeletal muscle, reduction of calories also affects the skeletal muscle metabolome.

Sex and strain response to fasting and calories

Sex and genetic background impact the response to CR in mice[21,22,26]; to determine if the distinct roles of calorie and fasting we observed in B6M was conserved across different sexes and strains, we examined female C57BL/6J (B6F) mice, and male and female DBA/2J (D2M and D2F) mice (Extended Figs. 6–8). These strains have different metabolic responses to once-daily CR, but CR extends the lifespan of both strains and sexes[21].

All three dietary regimens had similar effects on the body composition of B6M and D2M mice (Figs. 1B–E and Extended Figs. 7B–E). While female B6F and female D2F mice gained less weight on all of the reduced calorie regimens, Diluted AL-fed female mice did not gain fat mass nor adiposity (Extended Figs. 6A–D, 8A–D), suggesting there may be a sexually dimorphic effect of fasting (or the lack thereof) on fat storage. Glucose tolerance was improved by the reduced calorie regimens in all sexes and strains, with the exception of B6F fed the classical CR diet (Fig. 1F, Extended Figs. 6F, 7F, 8F and Supplementary Fig. 2A). While the non-responsiveness of B6F was somewhat surprising, these findings were in line with our previous observation that the effect of CR on glucose tolerance is stronger in young males than in young female mice[7]. This was not due to increased insulin secretion (Supplementary Fig. 3).

Insulin sensitivity as assessed by insulin tolerance test using 0.5U/kg insulin was significantly improved only in B6M fed the classic CR diet, and B6F fed either the classic CR diet or the MF.cr diet (Fig. 1G, Extended Fig. 6G and Supplementary Fig. 2B). We did not observe improved insulin sensitivity in response to any of the restricted diets for DBA/2J mice of either sex under these conditions (Extended Figs. 7G and 8G), exemplifying the genetic variation in response to insulin between strains[38]. As these mice were less responsive to insulin, after 14 weeks on diet, we challenged both male and female DBA/2J with a higher dose of insulin (0.75U/kg) in order to uncover differences between the diet regimens. We observed improved insulin sensitivity in D2F mice fed the classic CR diet, but not in D2M mice (Supplementary Fig. 2B). In all sexes and strains, mice fed the Diluted AL diet did not have significantly improved insulin sensitivity, despite the reduction in caloric intake. Interestingly, Diluted AL group had the smallest HOMA-IR value for B6F and D2M (Supplementary Fig. 3). These data demonstrate that sex and strain impact the effect of different CR regiments on glucose homeostasis.

Using metabolic chambers, we determined the RER and energy expenditure and calculated substrate utilization of all sexes, strains, and diet groups. All mice fed a classic CR diet had similar RER patterns to that of B6M, rapidly rising above 1.0 following refeeding and then falling to ~0.7–0.8 during the dark cycle (Fig. 1H and Extended Figs. 6H, 7H, 8H). While all mice fed the MF.cr diet had similar RER curves to classic CR-fed mice, all mice fed the Diluted AL diet had RER curves that overlapped those of the AL group (Extended Figs. 6H, 7H, 8H). As in B6M, CR and MF.cr diets increased fatty acid oxidation in D2M and D2F mice; B6F fed either one of these diets had FA oxidation indistinguishable from AL-fed controls (Fig. 1I, Extended Figs. 6I, 7I, 8I), suggesting that the strain and sex specific responses to CR regimens extends to fat metabolism. In contrast, fatty acid oxidation was not increased in Diluted AL-fed mice of any sex or strain.

All mice consuming fewer calories had decreased energy expenditure relative to their AL-fed counterparts; this effect was independent of both fat-free (lean) mass and body weight (Fig. 1J, Extended Figs 6J, 7J, 8J, and Supplementary Fig. 4).While all restricted groups of C57BL/6J and DBA/2J males had similar energy expenditure, female mice of both strains fed the Diluted diet had lower energy expenditure compared to both CR and MF.cr-fed mice (Extended Figs. 6J, 7J). These results suggest that fasting is responsible for the altered fuel

utilization of CR-fed animals, while the reduction in calories is responsible for the decreased exergy expenditure.

The physiological responses to these restricted paradigms were differentially regulated by strain and sex. To visualize the overall response, we plotted 17 phenotypes calculated relative to the AL Control. We first plotted how each individual sex/strain of mice responded to the three dietary regimens (Fig. 2A–D); secondly, we plotted how all four strains responded to each individual diet (Fig. 2E–G). To identify statistically significant interactions of sex, strain and diet, we performed multivariate statistical analyses on the 17 phenotypes. We used two-way ANOVA corrected for multiple comparisons by false discovery rate (FDR) using two-stage linear step-up procedure of Benjamini, Krieger and Yekutieli; the q values (FDR) and individual P values are shown in Supplementary Table 6. The majority of the phenotypic outcomes were both strain and sex dependent. In particular, D2F exhibited higher insulin sensitivity than D2M, and B6F exhibited higher insulin sensitivity than D2F. For fatty acid oxidation there was a sex-diet interaction for DBA/2J mice, and a strain-diet interaction for both sexes. When total energy expenditure was evaluated against each strain and sex with ANCOVA, there were only strain differences for AL, Diluted AL, and MF.cr-fed mice. However, there were both strain and sex interactions for CR-fed mice.

Overall, there was little difference with strain or sex when only calories were restricted (Fig. 2H). As fasting duration increased, we observed an increasing number of sex and strain differences (Figs. 2I–J). Our data support the idea that each sex and strain respond to a CR diet uniquely as a result of sex and strain-specific responses to prolonged fasting.

Fasting recapitulates the metabolic effects of a CR diet

We next wanted to examine the possibility that fasting is sufficient to recapitulate the metabolic and molecular effects of a classical once-per-day CR diet. We designed a fifth feeding paradigm, TR.al, in which B6M mice were entrained to consume approximately the same quantity of food as *ad libitum* fed mice within 3 hours (Fig. 3A, Extended Fig. 9A), following which they were fasted for the remaining 21 hours of each day.

We found that both classical CR-fed mice and TR.al-fed mice had reduced overall weight and fat mass gain during the 16 weeks of the study, despite the similar calorie intake of AL and TR.al-fed mice (Fig. 3B, Extended Figs. 9A–E, and Supplementary Table 7). Additionally, TR.al-fed mice had improved glucose tolerance and insulin sensitivity after 9–10 weeks (Figs. 3C–D). These early improvements in glucose homeostasis were independent of significant difference in weight and adiposity, which only diverged after 12 weeks on diet (Extended Figs. 9B–E). Glucose tolerance and insulin sensitivity were similarly improved after 13–14 weeks on the diets (Extended Figs. 9F–G), and was not the result of increased insulin secretion (Extended Figs. 9H–J). These results demonstrate that prolonged fasting is sufficient to improve body composition, glucose tolerance and insulin sensitivity.

We utilized metabolic chambers to determine substrate utilization and energy expenditure. As previously shown, we found that classic CR-fed mice exhibited two distinct phases of fuel selection following feeding, with high lipogenesis (RER > 1.0) following feeding, and

dependence upon lipid oxidation (RER < 0.8) during the dark cycle, and an overall increase in FA oxidation (Figs. 3E–F). TR.al mice were essentially indistinguishable from classic CR-fed mice, with overlapping RER curves and similar increases in FA oxidation (Figs. 3E–F). The CR and TR.al groups both demonstrated decreased total energy expenditure relative to AL-fed mice that was independent of lean (fat-free) mass and body weight (Supplementary Fig. 5).

Almost all of the metabolic phenotypes of CR-fed mice are also observed in TR.al-fed mice (Fig. 3G). Additionally, when comparing all the feeding paradigms examined for B6M mice, we observed that only mice subject to prolonged fasting, the CR and TR.al groups, showed improved insulin sensitivity, while any length of fasting was sufficient to increase FA oxidation (Fig. 3H). Together, these results demonstrate that fasting recapitulates the physiological response to CR, and is both necessary and sufficient for the metabolic response to CR.

Fasting recapitulates the molecular effects of a CR diet

We next performed transcriptomic profiling of liver and inguinal white adipose tissue (iWAT) of mice fed either an AL, CR, or TR.al diet. We identified a total of 2,700 genes in the liver and more than 1,800 genes in iWAT that were differentially expressed ($q < 0.05$) in either CR or TR.al-fed mice relative to AL-fed mice (Fig. 4A–C, Supplementary Tables 8–9). A large fraction of these genes was altered in the same direction by both CR and TR.al-feeding (Fig. 4B); and over 90% of the differentially expressed genes (DEGs) were the same in iWAT and liver of CR and TR.al animals (Fig. 4C).

We next took an unbiased approach in identifying functionally enriched pathways by constructing gene-set networks with NetworkAnalyst[39–43]. DEGs were assigned as “seed” proteins and pathways were constructed with the known interactions of the seed protein with other proteins curated from a large protein-protein interaction (PPI) database (Figs. 4D–E). From this we identified likely candidate pathways mediating these responses by limiting pathway hits with enrichment p-values of <0.05 which were calculated with the hypergeometric test – enrichment analysis test that calculates for significant overlap between genes and ranked by their p-value.

More pathways were altered in iWAT than in the liver. We identified 25 upregulated pathways in iWAT that were functionally enriched in tissues from both CR and TR.al-fed mice (Fig. 4F). In liver, we identified 5 upregulated and 5 downregulated pathways that were functionally enriched by both diets (Fig. 4G). Additionally, some pathways were enriched in tissues for both CR and TR.al-fed mice, but reached statistical significance only for one diet, such as mTOR signaling pathway in iWAT (Fig. 4F) or PPAR signaling in liver (Fig. 4G). Lastly, we examined the similarities of enriched pathways between iWAT and liver. We identified six pathways upregulated in both tissues by both CR and TR.al diets – “Insulin signaling pathway”, “PPAR signaling pathway”, “Fatty acid biosynthesis”, “Circadian rhythm”, “Metabolic pathways”, and “Fatty acid metabolism” (Fig. 4F–G). We also identified two additional pathways that were upregulated in both tissues by TR.al only – “TGFβ signaling pathway” and “Longevity Regulating Pathway” (Fig. 4F–G). Finally, we found two pathways that were regulated in opposite directions in liver and iWAT by a TR.al

diet – “Signaling pathways regulating pluripotency of stem cells” and “MAPK signaling pathway” (Fig. 4F–G).

Fasting is necessary for CR to improve health and longevity

In order to understand the requirement for fasting in the effects of a CR diet on aging, we placed 20-week-old C57BL/6J male mice on either AL, Diluted AL or CR diets (Fig. 5A), and measured weight, body composition, glucose homeostasis, gut integrity, and frailty as the animals aged (Figs. 5 and Extended Fig. 10). As we expected, mice fed the classical CR diet ceased to gain weight, fat mass, and lean mass, and maintained a lower adiposity than AL-fed controls (Fig. 5B). In contrast, Diluted AL-fed mice had an initial reduction in body weight and fat mass and started to steadily lose lean mass at 9 months of age (Fig. 5B, Extended Fig. 10A, and Supplementary Table 10). To determine if cellulose in the Diluted AL diet impairs the absorption of energy-yielding nutrients, we assessed the gross energy in diet consumed and feces excreted by bomb calorimetry of 19-month old mice. Diluted AL-fed mice ate more and had increased fecal output; when accounting for the amount of cellulose consumed, Diluted AL-fed mice absorbed digestible macronutrients similarly to AL-fed mice (Extended Fig. 10B). We additionally checked if gut barrier integrity were affected by the Diluted AL diet with fluorescein isothiocynate-dextran (FITC-Dextran 4kDa) in 20-month-old mice. While Diluted AL-fed animals had the same level of permeability as the AL, CR-fed animals had improved gut barrier integrity (Extended Fig. 10C).

We assessed glucose and insulin tolerance as the mice aged; both diets improved glucose tolerance (Figs. 5C and 5E). In contrast, insulin sensitivity was only improved in the classical CR-fed group (Figs. 5D and 5F). As in young animals, classical CR-fed mice displayed a distinctive RER curve, with a rapid induction of lipogenesis (RER > 1.0) following refeeding, and a low RER throughout the night (Fig. 5G). We calculated that CR-fed mice utilized fatty acids as a fuel source significantly more throughout the day compared to other groups (Fig. 5H). CR and Diluted AL groups both demonstrated decreased total energy expenditure relative to AL-fed mice that was independent of non-fat mass or total body weight with no significant differences in activity between groups (Supplementary Fig. 6).

We assessed the frailty of AL, Diluted AL, and CR-fed mice as they aged. As expected[7,44], frailty was significantly lower in CR-fed mice as they aged (Fig. 6A). In contrast, frailty was not reduced in Diluted AL-fed mice (Fig. 6A). Intriguingly, the specific deficits of AL-fed and Diluted AL-fed mice that contributed to their equivalent frailty varied, with Diluted AL-fed mice developing kyphosis, and AL mice having declining grip strength and body composition (Figs. 6B–E). The quality of the coat condition and fur color were diminished in both AL and Diluted AL mice, while CR mice retained a healthy coat (Figs. 6F–G). Additionally, we examined if fasting was required for cognition and memory by testing novel object recognition[45]. Short-term memory was not improved in either Diluted AL-fed or CR-fed mice; however, classic once-per-day CR feeding, but not a Diluted AL diet, improved long-term memory (Figs. 6H–I), suggesting that fasting may play a role in the effects of a CR diet on cognition.

Finally, we analyzed the survival of the mice on the three different diets as they aged. While classic once-per day CR feeding extended lifespan by about 20% (AL vs CR, median lifespan 850 vs 1022, $p < 0.0001$ vs AL, log-rank sum test), consumption of the Diluted AL diet decreased lifespan by 9% (AL vs. Diluted AL, median lifespan 850 vs. 776 days, $p < 0.0001$ vs. AL, log-rank sum test) (Fig. 6J and Supplementary Table 11). Additionally, CR delayed the onset of cancer compared to AL, while the incidence of cancer in Diluted AL-fed mice was low, perhaps due to their shorter lifespan (Fig. 6k). In combination, our data suggest that fasting is required for the geroprotective effects of CR on frailty, cognition, and lifespan (Fig. 6L).

Discussion

The mechanisms by which CR promotes healthspan and longevity have remained elusive for decades. Most CR studies have overlooked the fact that a traditional once-per-day feeding regimen alters feeding behavior[15,16]. Meal feeding, which imposes a fasting period, was recently shown to extend lifespan without restricting caloric intake[20,46], which suggested to us that the fasting period collaterally imposed by a conventional once-per-day CR feeding regimen might be a critical and hitherto overlooked physiological mechanism contributing to the effects of CR.

We tested this hypothesis by using a novel series of feeding paradigms. We found that a reduction of calories without the imposition of a prolonged fast improves glucose tolerance and body composition. However, prolonged fasting was necessary for CR to improve insulin sensitivity, a key physiological hallmark of the CR response in mammals; alter fuel utilization patterns and increase fatty acid oxidation; and reduce age-related frailty[6,7,16,44,47,53]. Of note, we assessed insulin sensitivity via I.P. administration of insulin, which most directly measures insulin-stimulated glucose uptake; future research using clamps may be useful in thoroughly assessing the insulin sensitivity of other tissues including the liver.

C57BL/6J male mice in which calorie intake was reduced without fasting via *ad libitum* feeding of a low-energy diet did not show the anticipated reduction in age-related frailty, and had a reduced lifespan. Our findings align with the results of other labs[8], and with the results of our molecular analysis of the liver, which likewise showed that restriction of calories without fasting had a distinct and muted impact on metabolites and histone PTMs as compared to mice fed CR once-per-day. We observed changes in multiple methionine metabolites, and while it is difficult to directly compare metabolomics data across studies, other groups have seen similar changes[21,46,49–52]. In agreement with another study of mice fed the same chow we used[21,46], we observed that CR increased levels of leucine and isoleucine in the liver.

Our use of a diet diluted with indigestible cellulose (Diluted AL) is a limitation of the present work, as the large bulk of fiber in this diet may have affected the gut microbiome and impacted the metabolic effects we observed. While the diet did not affect macronutrient absorption or gut integrity, absorption of specific micronutrients was not investigated. We examined the effect of a more “normal” CR diet, delivered in multiple meals, (MF.cr), only

in our short-term studies. Future studies examining different MF.cr lengths in longer studies, testing multiple feeding times, and examining macro- and micro-nutrient absorption will permit a more complete understanding of how the length of time between meals contributes to the effects of a CR diet. This may also clarify why some studies report positive effects of cellulose-diluted diets on lifespan[53], and explain why dilution of specific macronutrients extends the lifespan of other model organisms[14,54–56].

Not only is a fasting period necessary, but the imposition of a prolonged daily fast without reduced calories recapitulates the metabolic benefits and molecular effects of a CR diet in C57BL/6J male mice. Fasting improves glucose tolerance and insulin sensitivity, reduces adiposity, and increases fatty acid oxidation. At the molecular level, fasting and traditional CR had extremely similar and overlapping effects on gene expression, with high similarity in the pathways altered by fasting and CR. Fasting almost completely recapitulates the effects of CR in both liver and iWAT, both in terms of differentially expressed genes and in KEGG pathways. Notably, many of the KEGG pathways identified as altered by both fasting and CR have been previously implicated in the metabolic and geroprotective effects of a CR diet; these include PPAR, insulin, TGFβ and AMPK signaling, as well as multiple metabolic pathways involved in amino acid, carbohydrate, and fatty acid metabolism. Similar changes in amino acid metabolism, PPAR expression, TGFβ and insulin signaling have been found in recent metabolomic and transcriptomic studies of the effects of graded levels of CR[49,57,58]. Intriguingly, Circadian rhythm was identified as a significantly altered pathway upregulated by both CR and fasting in iWAT, and by CR in the liver. We speculate that the daily fasting of mice on a classical CR diet may promote health and longevity in part through the circadian synchronization of metabolic processes[59]. Taken together, our data demonstrates that prolonged fasting is sufficient to recapitulate the majority of the effects of CR at the molecular level in both liver and iWAT. Additional research will be required to determine the role of these various pathways, as well as circadian regulators, in the response to prolonged fasting and CR.

Our study was subject to limitations. First, while we performed our initial sufficiency studies in multiple strains and sexes of mice, our metabolomic and epigenetic analysis was limited to C57BL/6J male mice on just three dietary regimens. As the effects of dietary composition and CR are sex and strain dependent[21,22,60], investigating the effects in multiple sexes and strains is critical. Our detailed studies of the effects of fasting alone were confined to C57BL/6J males, as this group showed the greatest metabolic response to a CR diet; and we focused on just a few diets for logistical reasons. Finally, TR.al-fed mice had a small reduction in calorie intake relative to AL-fed mice. We consider it unlikely that this contributes significantly to the effects of a TR.al diet, but follow-up studies should minimize or eliminate this difference. Additional research will be required to determine if fasting is sufficient to recapitulate the metabolic, molecular and geroprotective effects of a CR diet in multiple strains and sexes as well as in genetically heterogeneous mice.

Our results are in broad agreement with a series of studies over the last decade that have demonstrated that a prolonged inter-meal interval has significant health benefits. Restricting feeding to 8–10 hours per day protects mice from diet-induced obesity and insulin resistance without reducing calorie intake, perhaps by promoting regular daily rhythms in fasting and

feeding[18,61]. In pre-diabetic humans, a recent randomized clinical trial found that restricting feeding to 6 hours per day improved insulin sensitivity and beta cell function without a reduction in calories or weight loss[62]. Several decades ago one study found that the time of delivery of a once-per-day classical CR diet, or delivery of a CR diet in multiple meals limited to the dark period, had similar effects on the lifespan of mice[24]. It was recently shown that single-meal feeding of mice, resulting in an approximately 11-hour fast between meals, extends lifespan and healthspan, although to a lesser extent than a once-per-day classical CR diet[20]. Conversely, mice fed a low-energy density diet *ad libitum* spend more time eating than mice fed higher energy-density diets *ad libitum*, and as we also observed in the present study, have a shorter lifespan[8]. Our results, which demonstrate that prolonged daily fasting without reduced calorie intake is sufficient to recapitulate both the metabolic impact and molecular profile of a CR diet, are in agreement with these results, and clearly demonstrate that a prolonged inter-meal interval can benefit both metabolic health and longevity.

CR extended the lifespan of non-human primates in a study conducted at the University of Wisconsin-Madison (UW)[63], but did not extend lifespan in a study conducted at the National Institute on Aging (NIA)[64]. Notably, NIA control animals were long-lived compared to any data in captivity, possible due to the relatively low caloric intake of these animals. In both studies, when accounting for food intake and weight, animals that ate less and weighed less had increased lifespan. Other differences between the UW and NIA studies includes the age at which CR was initiated and diet composition[65]. There were also differences in feeding behavior, with animals at UW animals fed one main meal in the morning with a smaller snack in the afternoon[66]; as they rapidly consumed both the meal and the snack in under an hour (personal communication, Dr. Ricki Colman), the animals spent the majority of the day in the fasted state. In contrast, NIA animals were fed twice a day[64]. These conditions may be comparable to the CR and MF.cr groups in our study. While there are improved biomarkers of health in humans subjected to CR[3], humans adhering to a CR diet typically eat multiple meals per day. If our findings apply to humans, sharply limiting the portion of the day during which food is consumed may maximize the healthspan and longevity benefits of CR, and may promote healthy aging without requiring a reduction in calorie intake.

Time-restricted feeding studies suggest this may be case[67,68], although caution is warranted in applying these results to humans. In mice, once-per-day CR feeding performed early in the dark cycle or early in the light cycle has equivalent effects on lifespan[24]. However, in humans, skipping breakfast is associated with an increased risk of atherosclerosis and mortality[69,70]. In humans eating one isocaloric meal per day, weight declined in a breakfast-only group while weight increased in a dinner-only group[71]. Other studies have observed beneficial effects of once-per-day evening feeding on fat mass, but negative effects on cholesterol, blood pressure, and glucose control in healthy adults[72,73], and reduced weight and blood glucose control in adults with type 2 diabetes fed in the midafternoon or later[74]. Understanding how when we eat, and not just how much we eat, and its impact on metabolic health and longevity in humans is clearly an important area for future research.

Our work challenges long-standing assumptions about CR, and as summarized in Figure 7, we find that collaterally imposed fasting is required for the metabolic, molecular, and

geroprotective effects of a CR diet. Our study has important implications for research into the mechanisms which underlie the effect of CR; for example, this may explain in part why different methods of dietary restriction in worms and flies rely on different molecular pathways[55]. Re-imagining model systems to incorporate periodic fasting may provide valuable new insights into how CR works. Additionally, while restricting calories has long been viewed as unsustainable, fasting is incorporated in many fad diets and religious traditions. If these results apply to humans, fasting alone may be able to recapitulate the benefits of a CR diet without the side effects. In conclusion, our work demonstrates that daily prolonged fasting has powerful health benefits and underlies many benefits of a CR diet in mice, and that while "you are what you eat," it is equally true that "you are when you eat."

Materials and Methods

Animals, Diets, and Feeding Regimens

All procedures were performed in conformance with institutional guidelines and were approved by the Institutional Animal Care and Use Committee of the William S. Middleton Memorial Veterans Hospital (Assurance ID: D16-00403) (Madison, WI, USA). Male and female C57BL/6J and DBA/2J mice (stock numbers 000664 and 000671) were purchased from the Jackson Laboratory (Bar Harbor, ME, USA) at 8 weeks of age and acclimated to the animal research facility for at least one week before entering studies. All animals were housed in a specific pathogen free (SPF) mouse facility with a 12:12 hour light/dark cycle maintained at 20°−22°C. All animals were placed on 2018 Teklad Global 18% Protein Rodent Diet for one week before randomization. At 10 weeks of age, mice were randomized to one of 5 diet groups: 1) AL, *ad libitum* diet: 2) CR, animals in which calories were restricted by 30%, and animals were fed once per day during the start of the light period; 3) MF.cr, animals in which calories were restricted 30%, and animals were fed three equal meals during the course of the 12 hour dark period using an automated feeder (F14 Aquarium Fish Feeder, Fish Mate)[75]; 4) Diluted AL, animals provided with *ad libitum* access to a low energy diet diluted with indigestible cellulose, which reduced calorie intake by ~30%; and 5) TR.al, a feeding paradigm where mice were entrained to rapidly consume an *ad libitum* portion of food. Animals fed an AL, CR, MF.cr and TR.al diet were fed 2018 Teklad Global 18% Protein Rodent Diet, Envigo Teklad. Animals fed a Diluted AL diet were fed Teklad 2018 with 50% Cellulose (TD.170950). A stepwise reduction in food intake by increments of 10% per week, starting at 20% was carried out for mice in the CR group. In this study we highlight CR regimen as a fasting model; therefore, we decided to feed these animals in the morning as it aligns best with the last feeding time point from the *ad libitum* fed animals and MF.cr. This feeding schedule is also widely used (e.g. by the NIA Aging Rodent Colony[23]), and the time-of-day at which feeding occurs has been shown to not affect the ability of CR to extend lifespan[24]. Mice in the TR.al group were entrained to eat comparably to the AL-fed group within a 3-hour period during the first two weeks, and food was always removed 3 hours after the start of feeding. Body weight and food intake were monitored weekly. Due to shredding behavior of Diluted AL, we performed a comprehensive food consumption where we measured average shredded food and food left in the hopper. We found an average of 23% of the food were shredded on the bed of the

cage. We accounted for this value to calculate for Diluted AL food consumption presented in this manuscript. CR and TR.al mice were fed daily at approximately 7:00 a.m. Animal rooms were maintained at 20°C – 22°C with 30%−70% relative humidity and a 12-hr light/dark cycle. The caloric intake of the mice in the AL group was calculated weekly to determine the appropriate number of calories to feed the mice in the CR and MF.cr groups. The caloric intake of the mice in TR.al were calculated daily to monitor food intake.

Metabolic Phenotyping

Glucose and insulin tolerance tests (GTT and ITT) were performed by fasting all mice overnight and then injecting either glucose (1 g/kg) or insulin (0.5U/kg or 0.75U/kg) intraperitoneally[7]. Glucose measurements were taken using a Bayer Contour blood glucose meter and test strips. Mouse body composition was determined using an EchoMRI Body Composition Analyzer. For assay of multiple metabolic parameters (O_2, CO_2, food consumption and activity tracking), mice were acclimated to housing in a Columbus Instruments Oxymax/CLAMS metabolic chamber system for ~24 hour, and data from a continuous 24-hr period was then recorded and analyzed. AL-fed and Diluted AL-fed mice had ad libitum access to their respective diets; MF.cr and CR-fed mice were fed once per day at the beginning of the light cycle as indicated in each figure.

Sacrifice and Collection of Tissues

Mice were sacrificed in either in the fasted or fed state after 16 weeks on diet. Mice sacrificed in the fasted were fasted overnight starting at 11 am and then sacrificed between 9 and 11 am the next morning. Mice sacrificed in the fed state were fed starting at 7 am and sacrificed 3 hours later. Following blood collection via submandibular bleeding, mice were euthanized by cervical dislocation and tissues (liver, muscle, iWAT, eWAT, BAT, and cecum) were rapidly collected, weighed, and then snap frozen in liquid nitrogen.

Transcriptional profiling and analysis

RNA was extracted from liver or iWAT using Trireagent according to the manufacturer's protocol (Sigma-Aldrich). The concentration and purity of RNA were determined by absorbance at 260/280 nm using Nanodrop (Thermo Fisher Scientific) and sent to UW Biotechnology Center for sequencing and data annotation. Heatmaps were created using Prism 8.0 with log2 transformed data. Networks were constructed using NetworkAnalyst (Version 2) by protein-protein interaction[39–43] and pathways were identified with functional enrichment analysis using gene sets from Kegg.

Liver Tissue Metabolite Extraction

M. musculus liver tissue was powdered in liquid nitrogen using a mortar and pestle. Powdered tissue was transferred to an individual 1.5 ml microcentrifuge Eppendorf tube and incubated with 1 ml −80°C 80:20 MeOH:H_2O extraction solvent on dry ice for 5 minutes post-vortexing. Tissue homogenate was centrifugated at maximum speed for 5 minutes at 4°C. Supernatant was transferred to a 15 ml tube after which the remaining pellet was resuspended in 0.8 ml −20°C 40:40:20 ACN:MeOH:H_2O extraction solvent and incubated on ice for 5 minutes. Tissue homogenate was again centrifugated at maximum

speed for 5 minutes at 4°C after which the supernatant was pooled with the previously isolated metabolite fraction. The 40:40:20 ACN:MeOH:H_2O extraction was then repeated. Next, equal volumes of pooled metabolite extract for each sample was transferred to a 1.5 ml microcentrifuge Eppendorf tube and completely dried using a Thermo Fisher Savant ISS110 SpeedVac. Dried metabolite extracts were resuspended in 85% ACN following microcentrifugation for 5 minutes at maximum speed at 4°C to pellet any remaining insoluble debris. Supernatant was then transferred to a glass vial for LC-MS analysis.

Skeletal Muscle Metabolite Extraction

Frozen skeletal muscle was pulverized using liquid nitrogen. Pulverized tissues (50 mg) were then homogenized in 1 mL cold (−20°C) aqueous HPLC-grade methanol with a single 5 mm metal bead using the Qiagen TissueLyser II. Disruption was carried out at 25 Hz for 30s. Homogenates were clarified by centrifugation, spiked with 13c-succinate, and submitted to the Mass Spec facility for targeted amino acid and TCA metabolite analysis.

Targeted LC-MS Metabolite Analyses

Each prepared metabolite sample was injected onto a Thermo Fisher Scientific Vanquish UHPLC using two distinct column/buffer combinations to maximize metabolome coverage. One combination utilized a Waters XBridge BEH Amide column (100 mm × 2.1 mm, 3.5 μm) coupled to a Thermo Fisher Q-Exactive mass spectrometer. For the Waters XBridge BEH Amide column, mobile phase (A) consisted of 97% H_2O, 3% ACN, 20 mM ammonium acetate, and 15 mM ammonium hydroxide pH 9.6. Organic phase (B) consisted of 100% ACN. Metabolites were resolved using the following linear gradient: 0 min, 85% B, 0.15 ml/min; 1.5 min, 85% B, 0.15 ml/min; 5.5 min, 40% B, 0.15 ml/min; 10 min, 40% B, 0.15 ml/min; 10.5 min, 40% B, 0.3 ml/min; 14.5 min, 40% B, 0.3 ml/min; 15 min, 85% B, 0.15 ml/min; 20 min, 85% B, 0.15 ml/min. The mass spectrometer was operated in positive ionization mode with a MS1 scan at resolution = 70,000, automatic gain control target = 3×10^6, and scan range = 60–186 m/z and 187–900 m/z. The remaining combination utilized a Waters Acquity UPLC BEH C18 column (100 mm × 2.1 mm × 1.7 μm). For the Waters Acquity UPLC BEH C18 column, mobile phase (A) consisted of 97% H_2O, 3% MeOH, 10mM TBA, 9mM acetate with a final pH = 8.1 – 8.4. Organic phase (B) consisted of 100% MeOH. Metabolites were resolved using the following linear gradient: 0 min, 95% B, 0.2 ml/min; 2.5 min, 95% B, 0.2 ml/min; 17 min, 5% B, 0.2 ml/min; 19.5 min, 5% B, 0.2 ml/min; 20 min, 95% B, 0.2 ml/min; 25 min, 95% B, 0.2 ml/min. The mass spectrometer was operated in negative ionization mode with a MS1 scan at resolution = 70,000, automatic gain control target = 1×10^6, and scan range = 85–1275 m/z. Individual metabolite data were called from data files using MAVEN version 2011.6.17 [76; 77] with retention times empirically determined in-house. Peak Area Top values were analyzed to determine metabolite expression. Heatmaps were created using Spyder Anaconda 3.

Lifespan and frailty assessment

8-week-old male C57BL/6J mice were obtained from The Jackson Laboratory and maintained on 2018 Teklad Global (18% Protein Rodent Diet, Envigo Teklad) diet until 4 months of age. The animals were then randomized into three groups (AL, Diluted AL or CR) of equivalent body weight. Mice on the Diluted AL diet were fed a formulation of

Teklad 2018 with 50% Cellulose (TD.170950), resulting in an approximate 30% decrease in calorie intake. The caloric intake and of the mice in the AL group was calculated weekly to determine the appropriate number of calories to feed the mice in the CR and MF.cr group. CR was implemented with gradual stepwise reduction in food intake by increments of 10% per week, starting at 20%, was carried out for CR mice. CR mice were fed daily at approximately 7:00 a.m.. Body weight and food intake were monitored every week until food intake was stabilized then monitored every other week. Mice were housed in a specific pathogen free (SPF) mouse facility with a 12:12 hour light/dark cycle maintained at 20°−22°C. Mice were euthanized for humane reasons if moribund, if the mice developed other specified problems (e.g. excessive tumor burden), or upon the recommendation of the facility veterinarian. Mice that developed rectal prolapse were treated with Anusol Plus daily; mice euthanized due to rectal prolapse without other health abnormalities were censored as of the date of euthanasia. Mice were censored as of the date of death if death was associated with a procedure.

Frailty was assessed using a 25-item frailty index based on the procedures defined by Whitehead et al.[69]. The items scored included alopecia, loss of fur color, dermatitis, loss of whiskers, coat condition, tumors, distended abdomen, kyphosis, tail stiffening, gait disorders, tremor, body condition score, vestibular disturbance, cataracts, corneal opacity, eye discharge/swelling, microphthalmia, nasal discharge, malocclusions, rectal prolapse, vaginal/uterine/penile prolapse, diarrhea, breathing rate/depth, mouse grimace score, and piloerection.

Bomb Calorimetry

We determined the caloric content of diet and feces of 19-month-old C57BL/6J male mice (diet implementation at 4-month-old) with an adiabatic bomb calorimeter (6200ea Oxygen Bomb Calorimeter; Parr Instrument Company). Bombs were calibrated using benzoic acid before use.

Intestinal barrier integrity

20-month-old C57BL/6J mice (diet implementation at 4-month-old) were fasted from food for 4 hours prior to and both food and water 4 hours after an oral gavage of 200 uL (50 mg/mL) FITC-Dextran (4kDa; Sigma-Aldrich). Blood was collected at 0, 30, 60, 120, and 240 minutes and fluorescence intensity were measured using an excitation wavelength of 493 nm and an emission wavelength of 517 nm.

Radar Charts

Values for radar chart were calculated for percent change from AL within specific strain and sex. The distance from the center represents the effect of each restricted diet vs. AL-fed mice (no difference = 100%). Data are presented as average of diet group per sex per strain.

Statistics

Data are presented as mean ± SEM unless otherwise specified. For box-plots, center line represents the median; box limits indicate the upper and lower 25th to 75th percentile, and whiskers extend to the smallest and largest data values. Analyses were performed using

Excel (2010 and 2016, Microsoft) or Prism 8 (GraphPad Software). Statistical analyses were performed using one or two-way ANOVA followed by Tukey-Kramer post hoc test specified in the figure legends. Other statistical details can also be found in the figure legends; in all figures, n represents the number of biologically independent animals. Sample sizes for longevity studies were determined in consultation with previously published power tables[79]. Sample sizes for metabolic studies were determined based on our previously published experimental results with the effects of dietary interventions[9], with the goal of having > 90% power to detect a change in area under the curve during a GTT ($p<0.05$). Data distribution was assumed to be normal, but this was not formally tested. Sample size for molecular analyses were chosen in consultation with core facility staff and experienced laboratory personnel.

Blinding—Investigators were blinded to diet groups during data collection whenever feasible, but this was not usually possible or feasible as cages were clearly marked to indicate the diet provided, mistakes, and the size and body composition of the mice was altered by strain and diet. However, blinding is not relevant to the majority of the studies conducted here, as the data are collected in numeric form, which is not readily subject to bias due to the need for subjective interpretation. Investigators were not blinded during necropsies, as the size and body composition of the mice was altered by strain and diet and group identity was therefore readily apparent.

Randomization—All studies were performed on animals or tissues collected from animals. Animals of each sex and strain were randomized into groups of equivalent weight prior to the beginning of the in vivo studies.

Extended Data

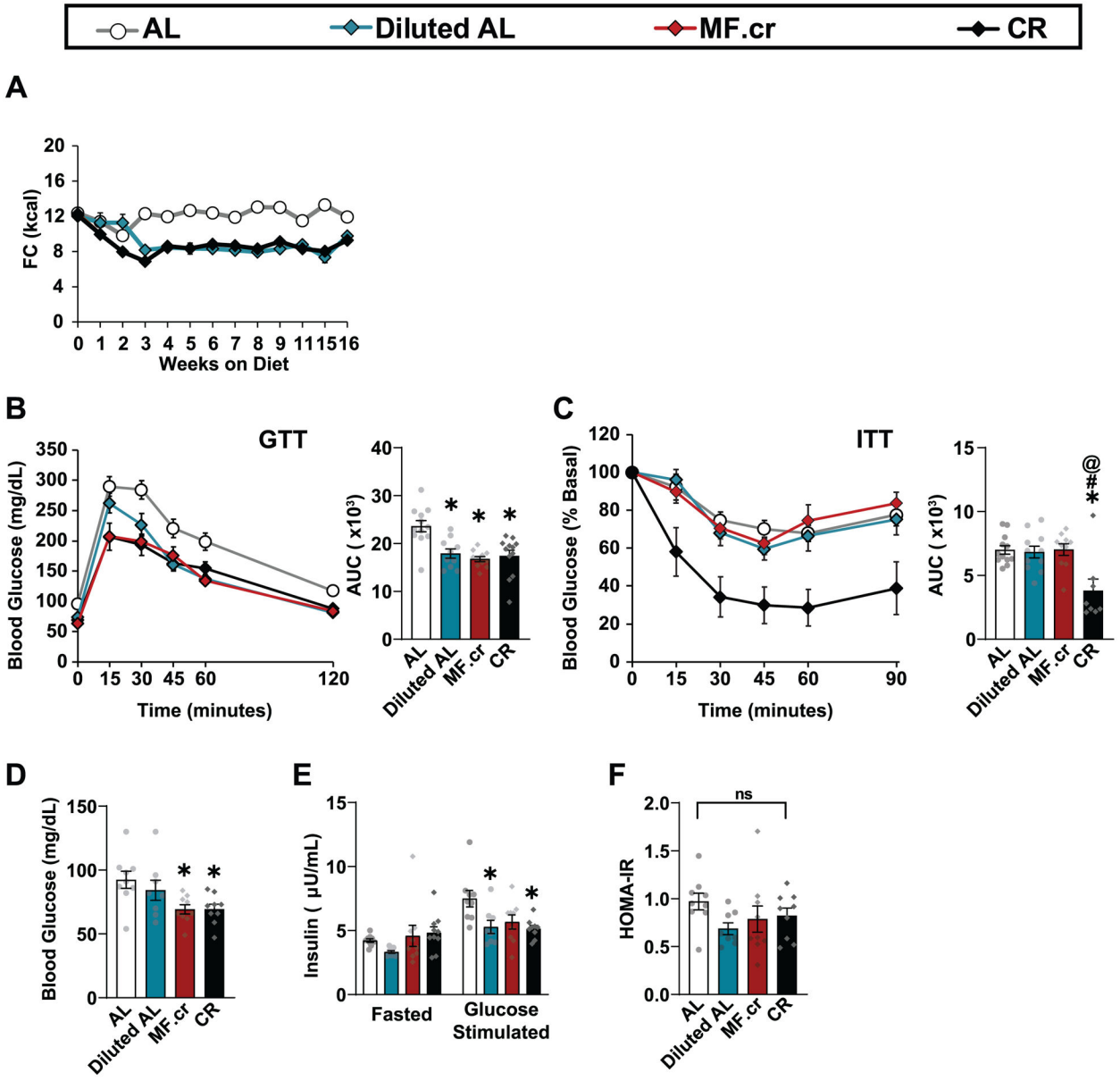

Extended Data Fig. 1. Additional measures of glucose homeostasis in male C57BL/6J mice

(A) Food Consumption (B) Glucose (AL, n = 12; Diluted AL, n = 10; MF.cr, n = 11; CR, n = 12 biologically independent mice) (C) and insulin (AL, n = 12; Diluted AL, n = 11; MF.cr, n = 10; CR, n = 8 biologically independent mice) tolerance tests after 13 or 14 weeks on the indicated diets. * symbol represents a significant difference versus AL-fed mice (p = 0.0009); # symbol represents a significant difference versus Diluted AL-fed mice (p = 0.0021); * symbol represents a significant difference versus MF.cr-fed mice (p = 0.0013) based on Tukey's test post one-way ANOVA. (D-F) Fasting blood glucose (D), fasting and glucose-stimulated insulin secretion (15 minutes) (E), and calculated HOMA-IR (F). (D-F) AL, n = 9; Diluted AL, n = 8; MF.cr, n = 9; CR, n = 9 biologically independent mice; *

symbol represents a significant difference versus AL-fed mice (Diluted AL, p = 0.0256; CR, p = 0.0127); insulin levels in fasted and glucose-stimulated states were analyzed separately. All data are represented as mean ± SEM.

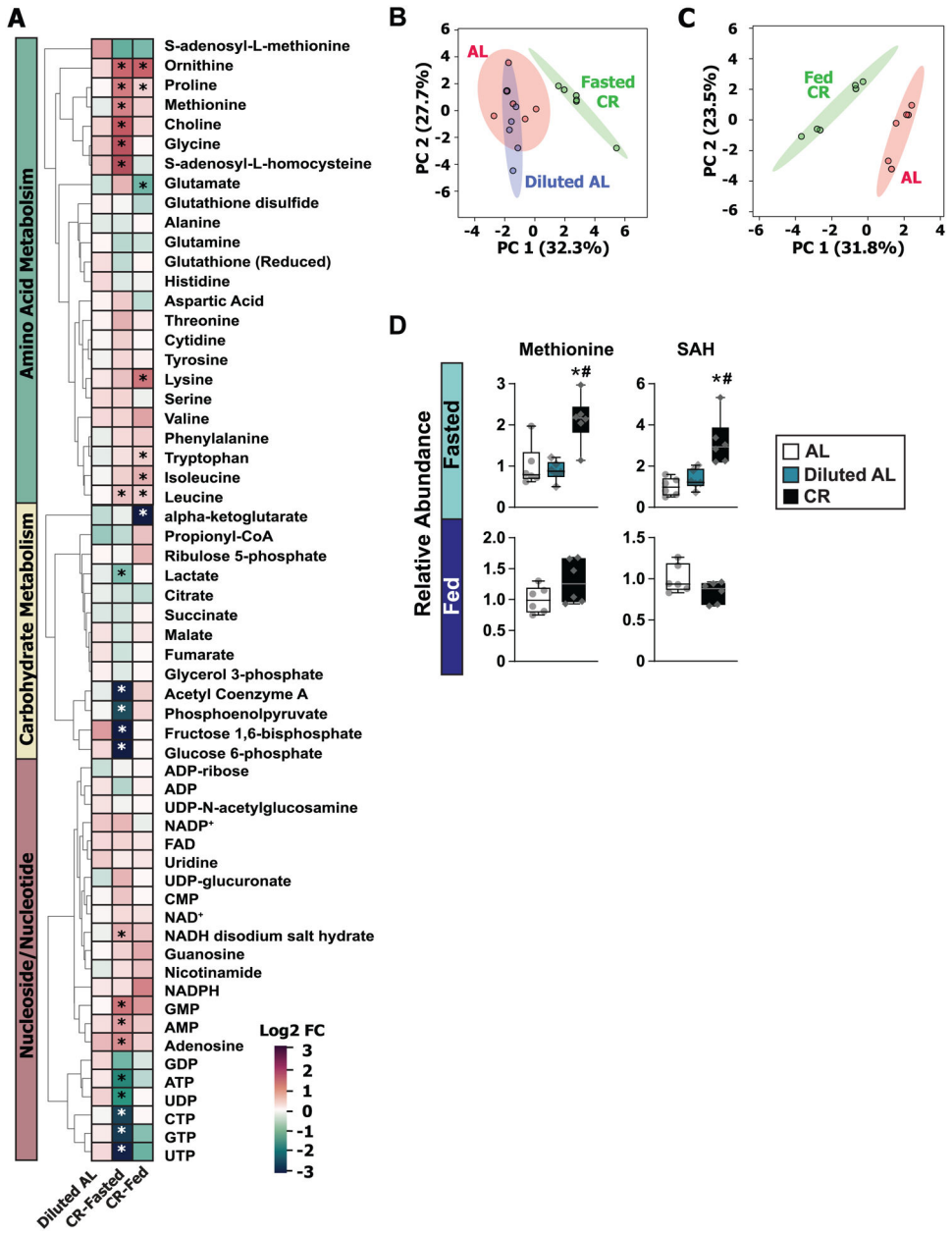

Extended Data Fig. 2. Fasting is required for CR-mediated reprogramming of the hepatic metabolome

Targeted metabolomics were performed on the livers of male C57BL/6J mice fed AL, Diluted AL and CR diets (n = 6 biologically independent mice per diet). A) Heatmap of 59 targeted metabolites, represented as $\log_2$-fold change vs. AL-fed mice. B) sPLS-DA of liver metabolomics with CR mice sacrificed in the fasted state. C) sPLS-DA of liver metabolomics with CR sacrificed in the fed state. (D) Relative abundance of methionine and

its metabolite S-Adenosyl-Homocysteine. * symbol represents a significant difference versus AL mice ($p \leq 0.0023$); # symbol represents a significant difference versus Diluted AL mice ($p \leq 0.0024$) based on Tukey's test post one-way ANOVA. Overlaid box plots show center as median and 25th-75th percentiles; whiskers represent minima and maxima.

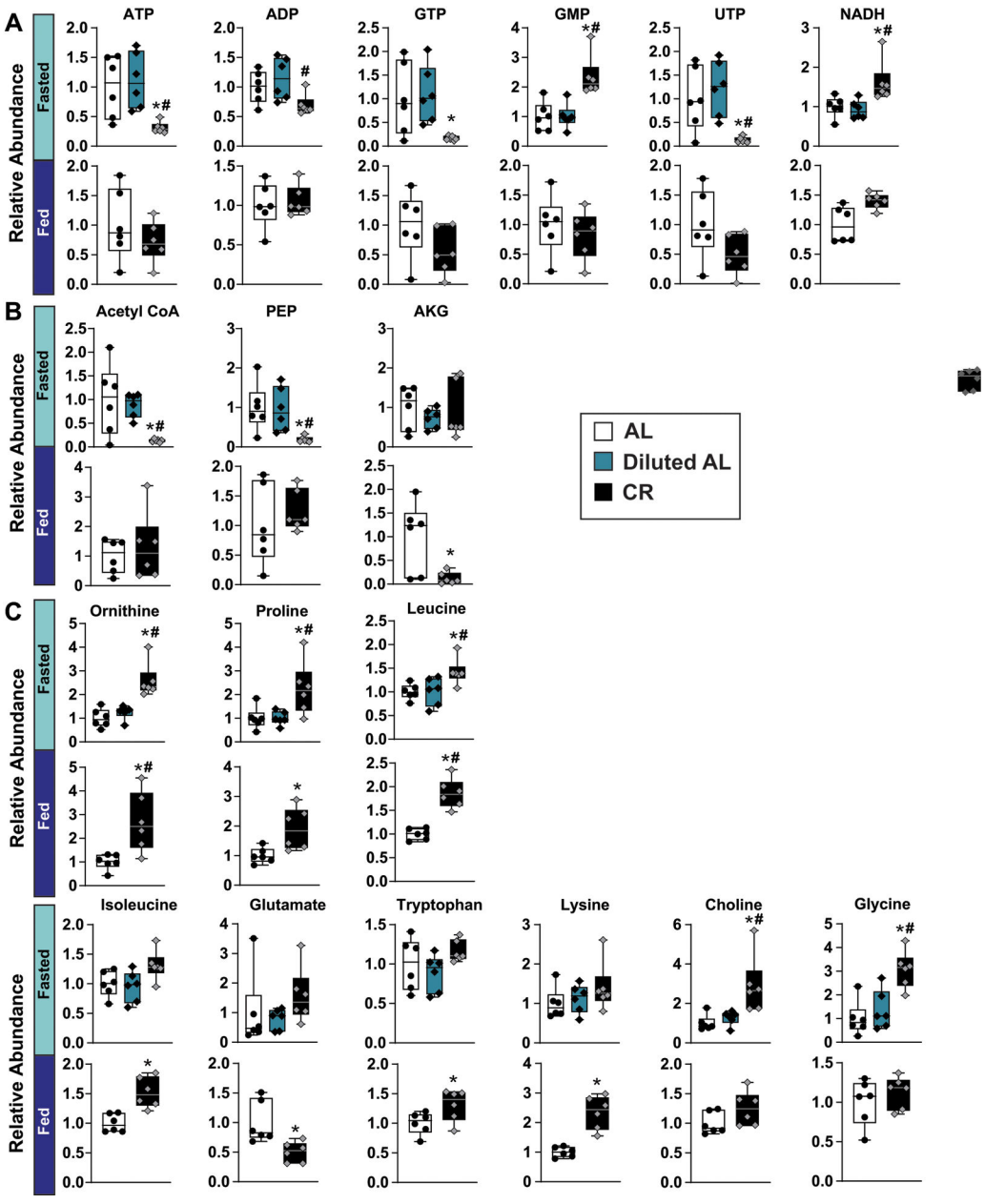

Extended Data Fig. 3. Additional hepatic metabolomic data

(A-C) Hepatic metabolites that showed a statistically significant difference during the fasted or fed state (n = 6 biologically independent mice per diet). A) Relative abundance of nucleotide/nucleoside metabolites. B) Relative abundance of TCA cycle metabolites. C) Relative abundance of amino acid metabolites. (A-C) * symbol represents a significant difference versus AL mice ($p \leq 0.05$); # symbol represents a significant difference versus

Diluted AL mice ($p \leq 0.05$) based on Tukey's test post one-way ANOVA. Overlaid box plots show center as median and 25th-75th percentiles; whiskers represent minima and maxima.

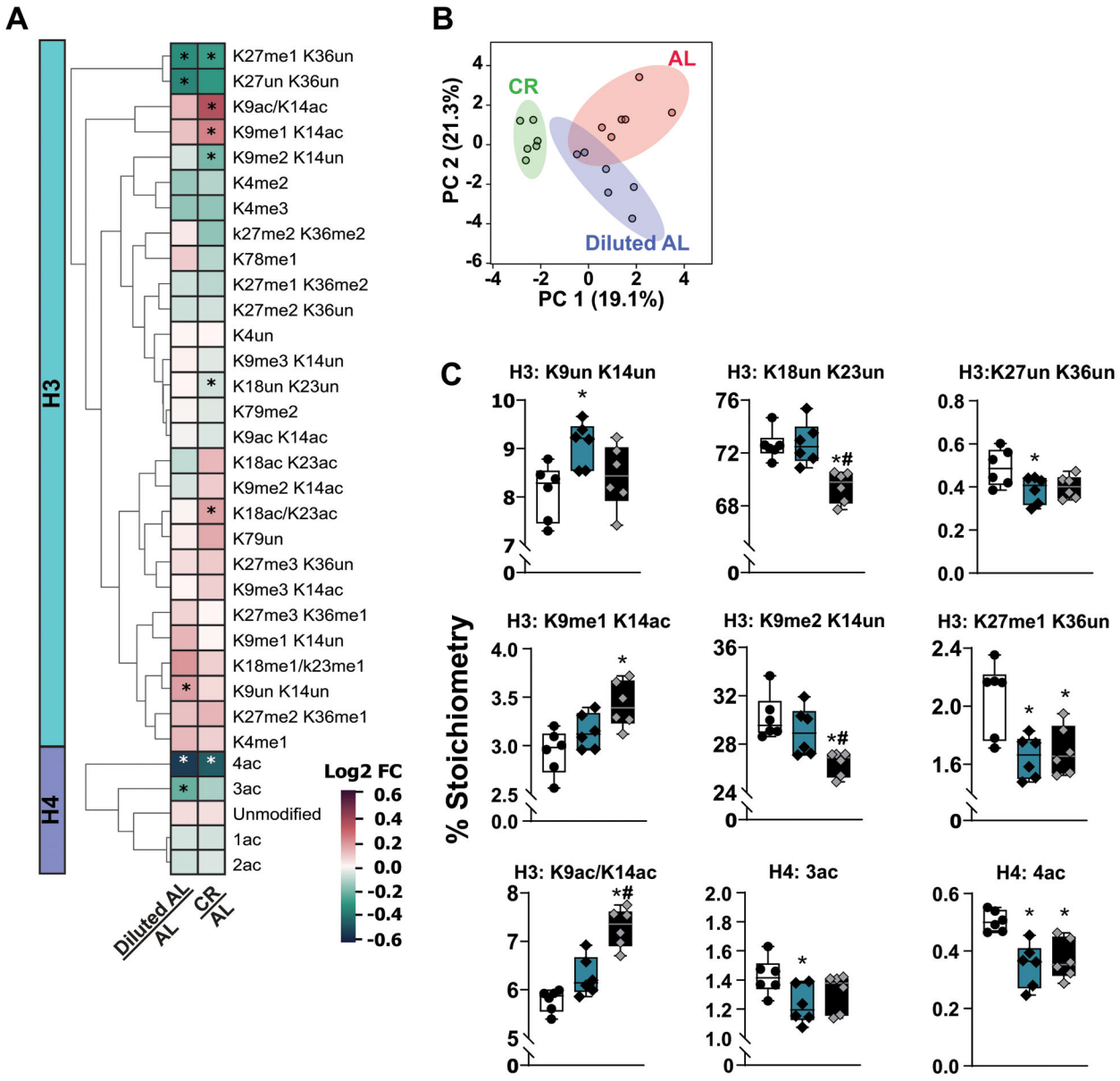

Extended Data Fig. 4. Fasting is required for CR-mediated reprogramming of the hepatic epigenome

Histone proteomics were performed on the livers of male C57BL/6J mice fed AL, Diluted AL and CR diets (n = 6 mice per group). A) Heatmap of histone H3 and H4 peptides represented as log2-fold change from AL. B) sPLS-DA of histone modifications. C) Statistically significant modified histones. (A-C) * symbol represents a significant difference versus AL mice ($p \leq 0.05$); # symbol represents a significant difference versus Diluted AL mice ($p \leq 0.05$) based on Tukey's test post one-way ANOVA. Overlaid box plots show center as median and 25th-75th percentiles; whiskers represent minima and maxima

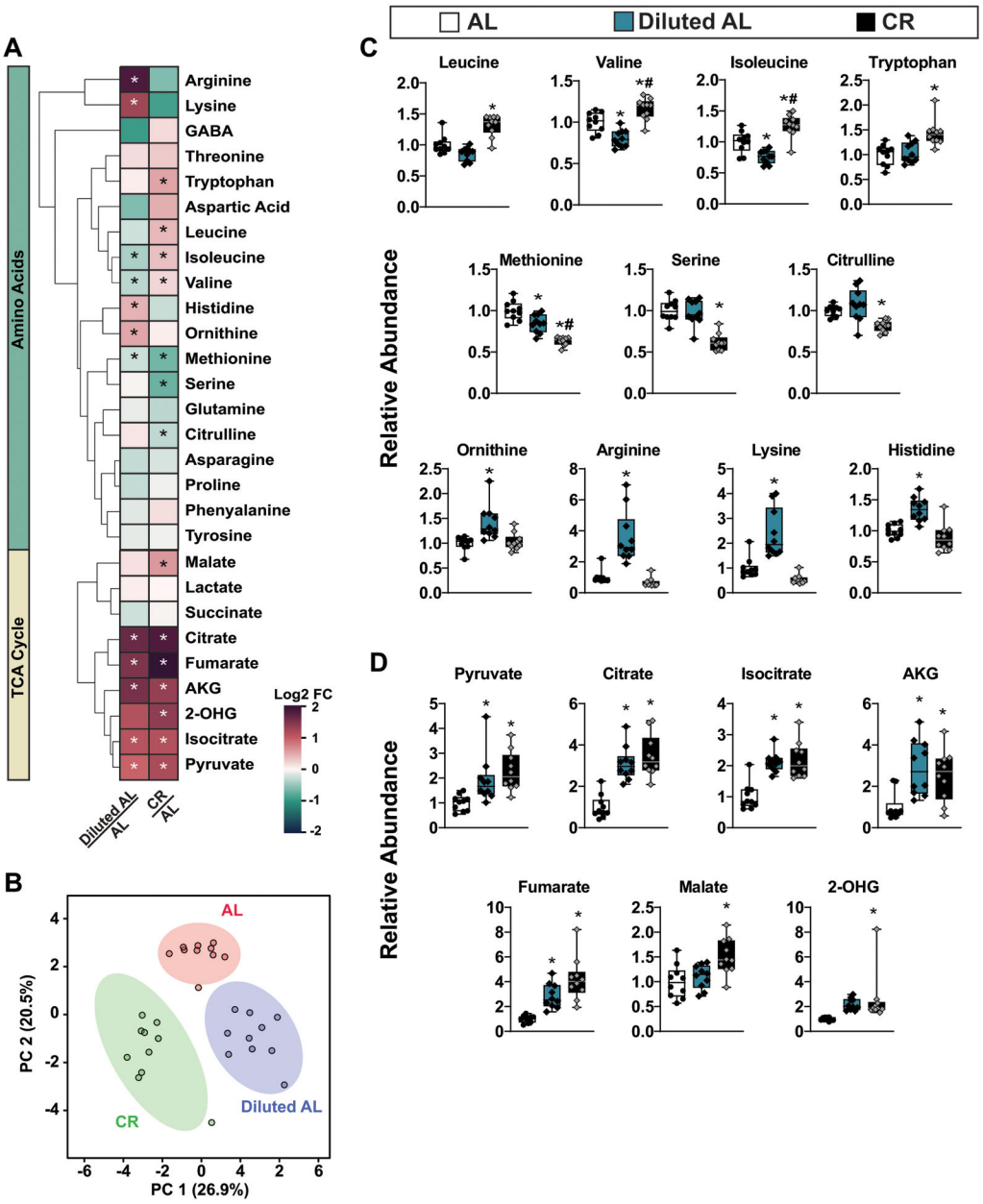

Extended Data Fig. 5. Metabolomic profile of skeletal muscle from AL, Diluted AL and CR mice

Targeted metabolomics were performed on skeletal muscle from male C57BL/6J mice fed AL, Diluted AL, and CR diets (n =10 biologically independent mice per diet). A) Heatmap of 28 targeted metabolites, represented as log2-fold change vs. AL-fed mice. B) sPLS-DA of skeletal muscle metabolites. C) Relative abundance of amino acid metabolites. D) Relative abundance of TCA cycle metabolites. (A-D) * symbol represents a significant difference versus AL mice ($p \leq 0.05$); # symbol represents a significant difference versus Diluted AL mice ($p \leq 0.05$) based on Tukey's test post one-way ANOVA. Overlaid box plots show center as median and 25th-75th percentiles; whiskers represent minima and maxima.

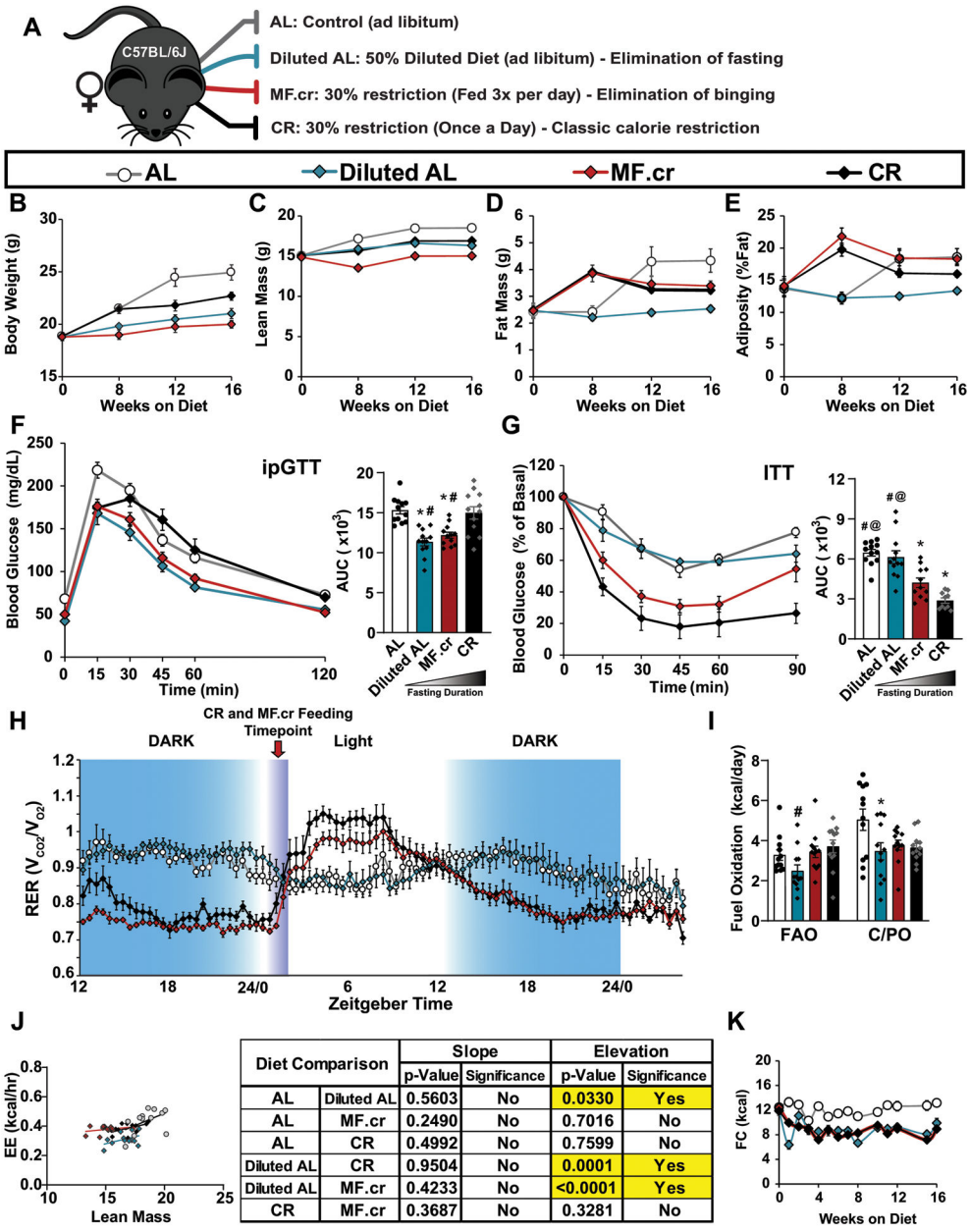

Diet Comparison		Slope		Elevation	
		p-Value	Significance	p-Value	Significance
AL	Diluted AL	0.5603	No	0.0330	Yes
AL	MF.cr	0.2490	No	0.7016	No
AL	CR	0.4992	No	0.7599	No
Diluted AL	CR	0.9504	No	0.0001	Yes
Diluted AL	MF.cr	0.4233	No	<0.0001	Yes
CR	MF.cr	0.3687	No	0.3281	No

Extended Data Fig. 6. The effect of three calorie restriction regimens on female C57BL/6J mice

(A) Outline of feeding regimens: AL, Diluted AL, CR and MF.cr. (B-E) Body composition measurement over 16 weeks on diet (AL, n = 12; Diluted AL, n = 10; MF.cr, n = 12; CR, n = 12 biologically independent mice); total body weight (B), lean mass (C), fat mass (D) and adiposity (E). (F-G) Glucose (n = 12 biologically independent mice per diet) (F) and insulin (AL, n = 12; Diluted AL, n = 12; MF.cr, n = 11; CR, n = 10 biologically independent mice) (G) tolerance tests after 9 or 10 weeks on the indicated diets. * symbol represents a significant difference versus AL-fed mice (Diluted AL, $p < 0.0001$; MF.cr, $p \leq 0.0012$, CR, $p < 0.0001$); # symbol represents a significant difference versus Diluted AL-fed mice (MF.cr, $p = 0.0019$; CR, $p \leq 0.0001$); @ symbol represents a significant difference versus MF.cr-fed mice (CR, $p = 0.0043$) based on Tukey's test post one-way ANOVA. (H-J)

Metabolic chamber analysis of mice fed the indicated diets. (H) Respiratory exchange ratio vs. time (n = 12 biologically independent mice per diet) (I) Fuel utilization was calculated for the 24-hour period following the indicated (arrow) refeeding time (n = 12 biologically independent mice per diet). * symbol represents a significant difference versus AL (Diluted AL, p = 0.0255); # symbol represents a significant difference versus Diluted AL (CR, p = 0.0274) based on Tukey's test post one-way ANOVA performed separately for FAO and C/PO). (J) Energy expenditure as a function of lean mass was calculated for the 24-hour period following the indicated (arrow) refeeding time (n = 12 biologically independent mice per diet, data for each individual mouse is plotted; slopes and intercepts were calculated using ANCOVA). K) Food consumption (AL, n = 12; Diluted AL, n = 12; MF.cr, n = 12; CR, n = 11–12). All data are represented as mean ± SEM.

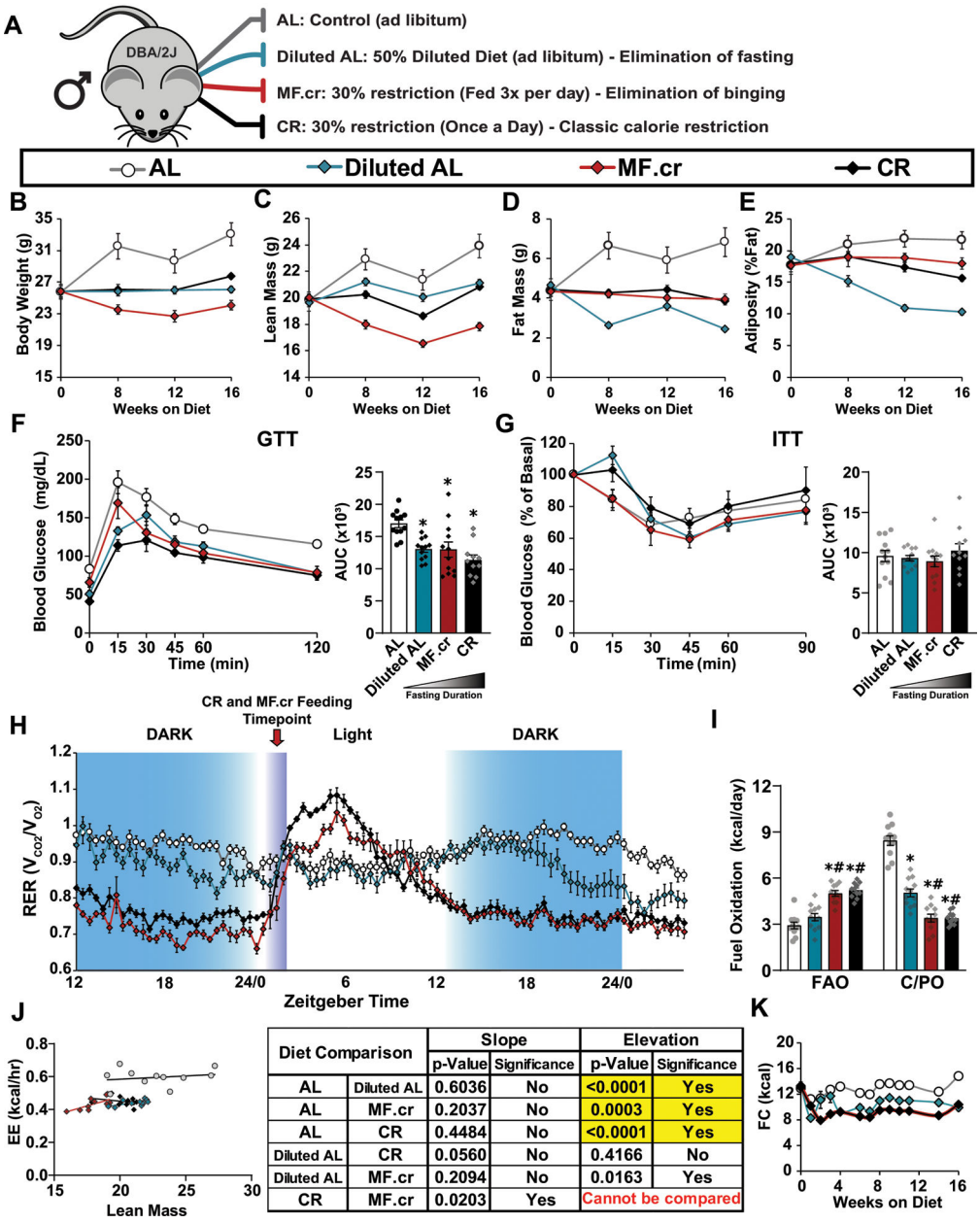

Diet Comparison		Slope		Elevation	
		p-Value	Significance	p-Value	Significance
AL	Diluted AL	0.6036	No	<0.0001	Yes
AL	MF.cr	0.2037	No	0.0003	Yes
AL	CR	0.4484	No	<0.0001	Yes
Diluted AL	CR	0.0560	No	0.4166	No
Diluted AL	MF.cr	0.2094	No	0.0163	Yes
CR	MF.cr	0.0203	Yes	Cannot be compared	

Extended Data Fig. 7. The effect of three calorie restriction regimens on male DBA/2J mice

(A) Outline of feeding regimens: AL, Diluted AL, CR and MF.cr. (B-E) Body composition measurement over 16 weeks on diet (AL, n = 11; Diluted AL, n = 11; MF.cr, n = 12; CR, n = 12 biologically independent mice); total body weight (B), lean mass (C), fat mass (D) and adiposity (E). (F-G) Glucose (AL, n = 12; Diluted AL, n = 12; MF.cr, n = 12; CR, n = 11 biologically independent mice) (F) and insulin (AL, n = 12; Diluted AL, n = 12; MF.cr, n = 12; CR, n = 11 biologically independent mice) (G) tolerance tests after 9 or 10 weeks on the indicated diets. * symbol represents a significant difference versus AL-fed mice (Diluted AL, p = 0.0059; MF.cr, p = 0.0052; CR, p < 0.0001) based on Tukey's test post one-way ANOVA. (H-J) Metabolic chamber analysis of mice fed the indicated diets. (H) Respiratory exchange ratio vs. time (AL, n = 12; Diluted AL, n = 11; MF.cr, n = 11;

CR, n = 11 biologically independent mice) (I) Fuel utilization was calculated for the 24-hour period following the indicated (arrow) refeeding time (AL, n = 12; Diluted AL, n = 11; MF.cr, n = 11; CR, n = 11 biologically independent mice). * symbol represents a significant difference versus AL (Diluted AL, $p < 0.0001$; MF.cr, $p < 0.0001$; CR, $p < 0.0001$); # symbol represents a significant difference versus Diluted AL (MF.cr, $p \leq 0.0002$; CR, $p \leq 0.0001$) based on Tukey's test post one-way ANOVA performed separately for FAO and C/PO). (J) Energy expenditure as a function of lean mass was calculated for the 24-hour period following the indicated (arrow) refeeding time (AL, n = 12; Diluted AL, n = 11; MF.cr, n = 11; CR, n = 11 biologically independent mice, data for each individual mouse is plotted; slopes and intercepts were calculated using ANCOVA). K) Food consumption (n = 12 biologically independent mice per diet). All data are represented as mean ± SEM.

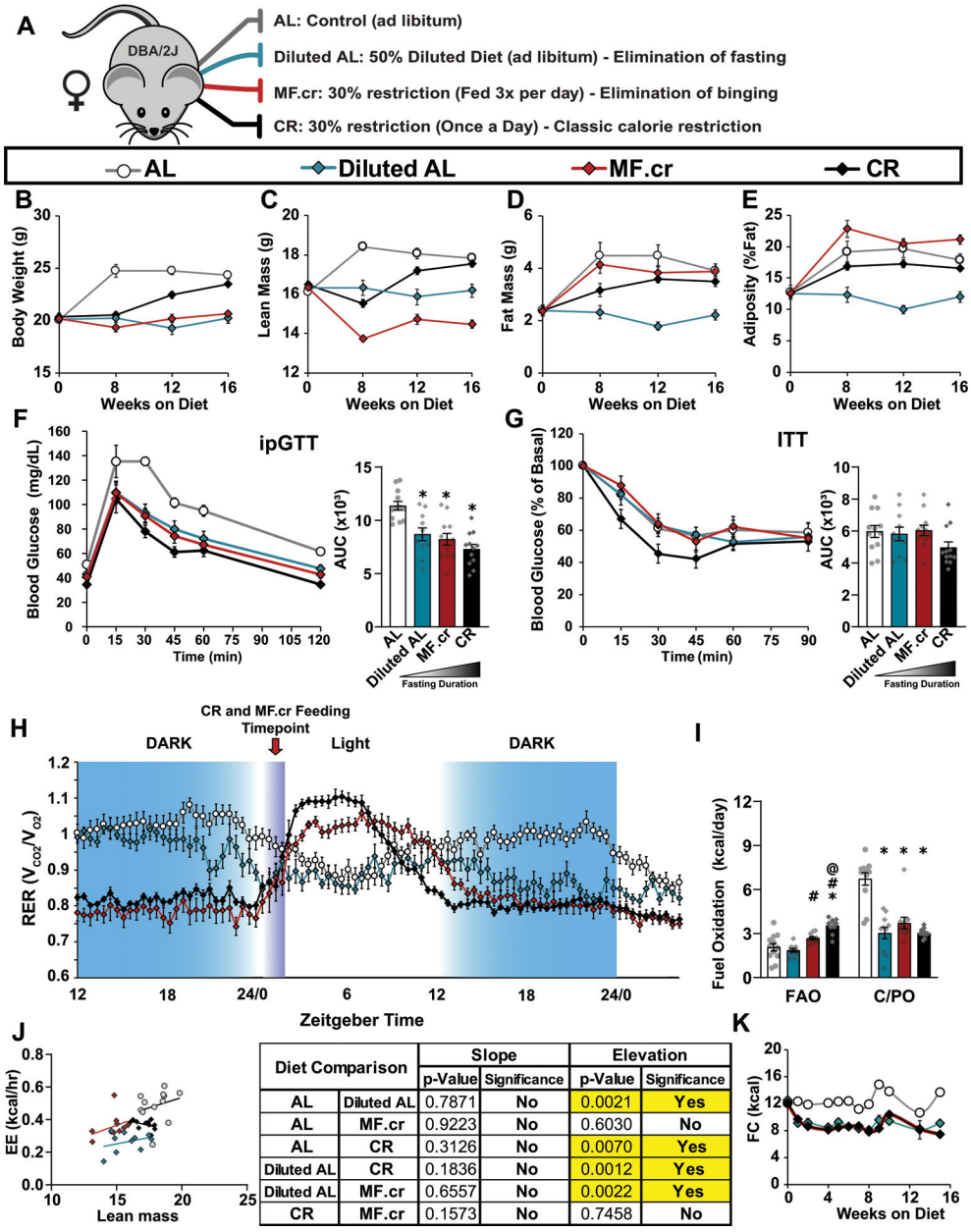

Diet Comparison		Slope		Elevation	
		p-Value	Significance	p-Value	Significance
AL	Diluted AL	0.7871	No	0.0021	Yes
AL	MF.cr	0.9223	No	0.6030	No
AL	CR	0.3126	No	0.0070	Yes
Diluted AL	CR	0.1836	No	0.0012	Yes
Diluted AL	MF.cr	0.6557	No	0.0022	Yes
CR	MF.cr	0.1573	No	0.7458	No

Extended Data Fig. 8. The effect of three calorie restriction regimens on female DBA/2J mice

(A) Outline of feeding regimens: AL, Diluted AL, CR and MF.cr. (B-E) Body composition measurement over 16 weeks on diet (AL, n = 12; Diluted AL, n = 7; MF.cr, n = 11; CR, n = 12 biologically independent mice); total body weight (B), lean mass (C), fat mass (D) and adiposity (E). (F-G) Glucose (AL, n = 12; Diluted AL, n = 11; MF.cr, n = 12; CR, n = 12 biologically independent mice) (F) and insulin (AL, n = 12; Diluted AL, n = 11; MF.cr, n = 12; CR, n = 12 biologically independent mice) (G) tolerance tests after 9 or 10 weeks on the indicated diets. * symbol represents a significant difference versus AL-fed mice (Diluted AL, p = 0.0033; MF.cr, p = 0.0003; CR, p < 0.0001) based on Tukey's test post one-way ANOVA. (H-J) Metabolic chamber analysis of mice fed the indicated diets. (H) Respiratory exchange ratio vs. time (AL, n = 11; Diluted AL, n = 11; MF.cr, n = 11;

CR, n = 10 biologically independent mice) (I) Fuel utilization was calculated for the 24-hour period following the indicated (arrow) refeeding time (AL, n = 11; Diluted AL, n = 11; MF.cr, n = 11; CR, n = 10 biologically independent mice). * symbol represents a significant difference versus AL (Diluted AL, $p < 0.0001$; MF.cr, $p < 0.0001$; CR, $p < 0.0001$); # symbol represents a significant difference versus Diluted AL (MF.cr, $p \leq 0.0128$; CR, $p < 0.0001$) ; @ symbol represents a significant difference versus MF.cr (CR, $p \leq 0.0074$) based on Tukey's test post one-way ANOVA performed separately for FAO and C/PO). (J) Energy expenditure as a function of lean mass was calculated for the 24-hour period following the indicated (arrow) refeeding time (AL, n = 11; Diluted AL, n = 11; MF.cr, n = 11; CR, n = 10 biologically independent mice, data for each individual mouse is plotted; slopes and intercepts were calculated using ANCOVA). K) Food consumption (AL, n = 12; Diluted AL, n = 7–12; MF.cr, n = 12; CR, n = 12 biologically independent mice). All data are represented as mean ± SEM.

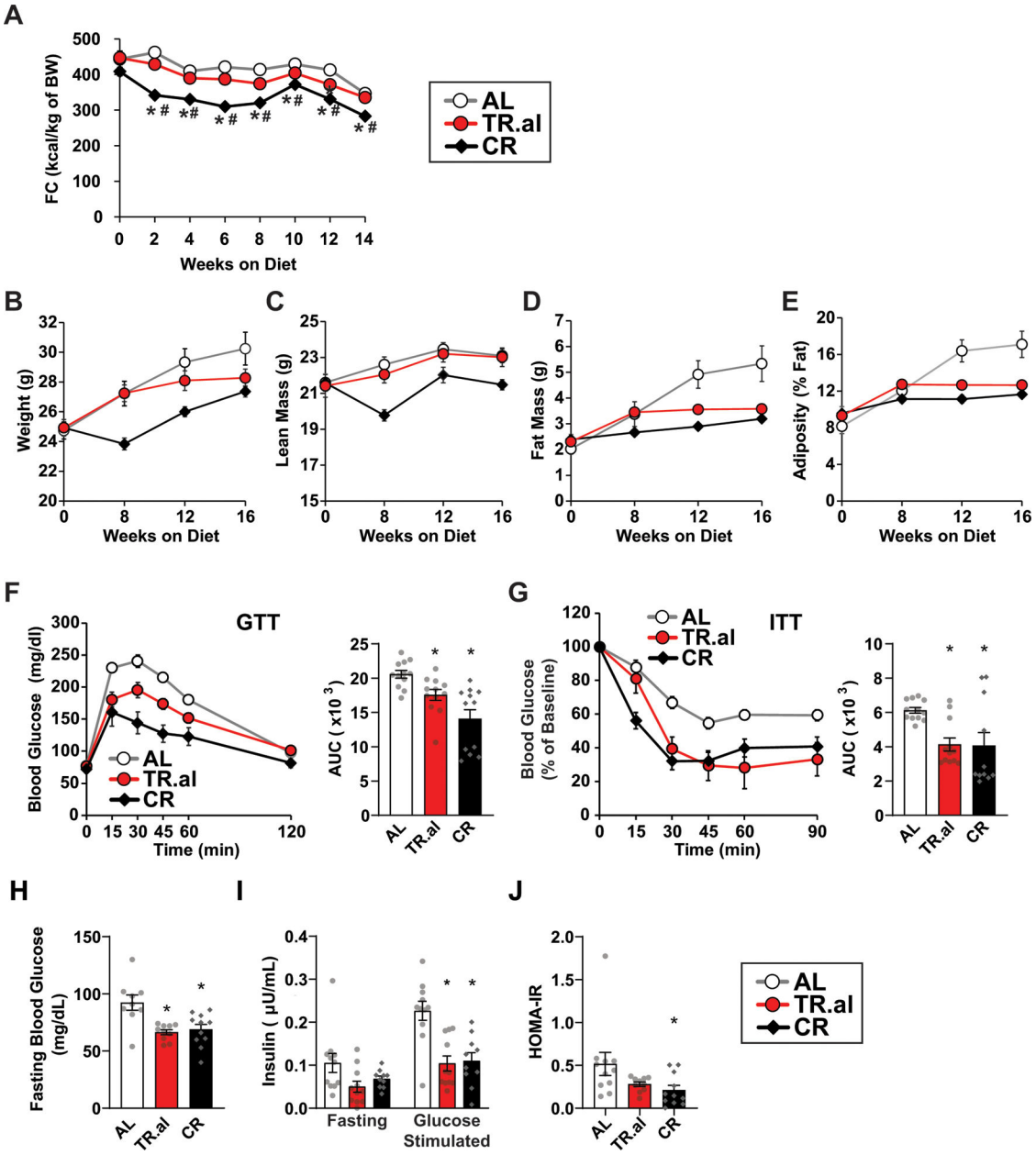

Extended Data Fig. 9. Additional data for C57BL/6J male mice fed CR or TR.al diets

A) Food consumption (n = 12 biologically independent mice per diet). B-E) Body composition (body weight, lean mass, fat mass and adiposity) of C57BL/6J male mice fed the indicated diets for 4 months (n = 12 biologically independent mice per diet; statistics on supplementary table 7). F-G) Glucose (n = 12 biologically independent mice per diet) (F) and insulin (AL, n = 12; TR.al, n = 12; CR, n = 11 biologically independent mice) (G) tolerance tests were performed after 13–14 weeks, respectively on the indicated diets. (H-J) Fasting blood glucose (H), fasting and glucose-stimulated insulin secretion (15 minutes) (I), and calculated HOMA2-IR (J) (AL, n = 12; TR.al, n = 11; CR, n = 12 biologically independent mice). * symbol represents a significant difference versus AL (TR.al, $p \leq 0.0018$; CR, $p \leq 0.0477$); # symbol represents a significant difference versus TR.al (MF.cr,

p ≤ 0.0187; CR, p = 0.0478) based on Tukey's test post one-way ANOVA. All data are represented as mean ± SEM.

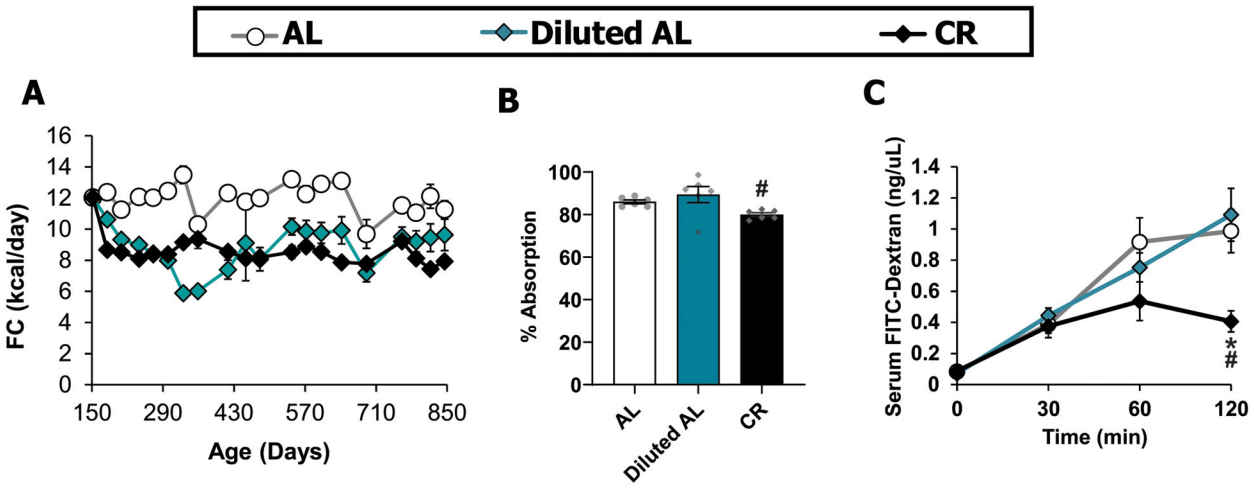

Extended Data Fig. 10. Food consumption, absorption and gut integrity

A) Food consumption (AL, n = 27–33; Diluted AL, n = 8–33; CR, n = 30–33 biologically independent mice). B) Food absorption calculation by bomb calorimetry of 19-month-old C57BL/6J male mice fed the indicated diets for 13 months (n = 6 biologically independent mice per diet) C) Gut integrity calculation by FITC-dextran of 20-month-old C57BL/6J male mice (n = 6 biologically independent mice per diet). * symbol represents a significant difference versus AL (CR, p = 0.0160); # symbol represents a significant difference versus Diluted AL (CR, p ≤ 0.0281) based on Tukey's test post two-way ANOVA) Data are represented as mean ± SEM.

Supplementary Material

Refer to Web version on PubMed Central for supplementary material.

ACKNOWLEDGEMENTS

We would like to thank all members of the Lamming lab, as well as Dr. Judith Simcox and Raghav Jain, for their valuable insights and comments. We thank Dr. Stephen Simpson and Dr. Samantha Solon-Biet for advice regarding animal care. We thank Dr. Tina Herfel (Envigo) for assistance with the formulation of the Diluted AL diet. We thank Dr. Michael Schaid for critical reading of the manuscript. The Lamming laboratory is supported in part by the NIH/NIA (AG050135, AG051974, AG056771, AG062328, and AG061635 to D.W.L.), NIH/NIDDK (DK125859 to D.W.L and J.M.D.) and startup funds from the University of Wisconsin-Madison School of Medicine and Public Health and Department of Medicine to D.W.L. Metabolomic and histone proteomic analysis was supported in part by the NIH grant R37GM059785 to J.M.D. and by a UAB Nathan Shock Center of Excellence in the Basic Biology of Aging (P30AG050886) Core Services Pilot Award to D.W.L. Bomb calorimetry was supported by S10OD028739 to C.L.E.Y and gut integrity analysis was supported in part by DK124696 to C.L.E.Y. H.H.P. is supported in part by a NIA F31 predoctoral fellowship (AG066311). C.L.G. is supported by a Glenn Foundation for Medical Research Postdoctoral Fellowship and was supported in part by a generous gift from Dalio Philanthropies. N.E.R. was supported in part by a training grant from the UW Institute on Aging (NIA T32 AG000213). S.A.H. was supported in part by a training grant from the UW Metabolism and Nutrition Training Program (T32 DK007665). Support for this research was provided by the University of Wisconsin - Madison Office of the Vice Chancellor for Research and Graduate Education with funding from the Wisconsin Alumni Research Foundation. This work was supported in part by the U.S. Department of Veterans Affairs (I01-BX004031), and this work was supported using facilities and resources from the William S. Middleton Memorial Veterans Hospital. The content is solely the responsibility of the authors and does not necessarily represent the official views of the NIH. This work does not represent the views of the Department of Veterans Affairs or the United States Government.

Data availability

The data that support the plots and other findings of this study are provided as a Source Data file or are available from the corresponding author upon reasonable request. RNA-sequencing data have been deposited with the Gene Expression Omnibus and are accessible through accession number GSE168262.

REFERENCES

1. Green CL, Lamming DW & Fontana L Molecular mechanisms of dietary restriction promoting health and longevity. Nat Rev Mol Cell Biol, doi:10.1038/s41580-021-00411-4 (2021).
2. Colman RJ et al. Caloric restriction reduces age-related and all-cause mortality in rhesus monkeys. Nature communications 5, 3557, doi:10.1038/ncomms4557 (2014).
3. Kraus WE et al. 2 years of calorie restriction and cardiometabolic risk (CALERIE): exploratory outcomes of a multicentre, phase 2, randomised controlled trial. Lancet Diabetes Endocrinol 7, 673–683, doi:10.1016/S2213-8587(19)30151-2 (2019). [PubMed: 31303390]
4. Belsky DW, Huffman KM, Pieper CF, Shalev I & Kraus WE Change in the Rate of Biological Aging in Response to Caloric Restriction: CALERIE Biobank Analysis. J Gerontol A Biol Sci Med Sci 73, 4–10, doi:10.1093/gerona/glx096 (2017). [PubMed: 28531269]
5. Das SK et al. Body-composition changes in the Comprehensive Assessment of Long-term Effects of Reducing Intake of Energy (CALERIE)-2 study: a 2-y randomized controlled trial of calorie restriction in nonobese humans. Am J Clin Nutr 105, 913–927, doi:10.3945/ajcn.116.137232 (2017). [PubMed: 28228420]
6. Balasubramanian P, Howell PR & Anderson RM Aging and Caloric Restriction Research: A Biological Perspective With Translational Potential. EBioMedicine 21, 37–44, doi:10.1016/j.ebiom.2017.06.015 (2017). [PubMed: 28648985]
7. Yu D et al. Calorie-Restriction-Induced Insulin Sensitivity Is Mediated by Adipose mTORC2 and Not Required for Lifespan Extension. Cell reports 29, 236–248 e233, doi:10.1016/j.celrep.2019.08.084 (2019). [PubMed: 31577953]
8. Solon-Biet SM et al. The ratio of macronutrients, not caloric intake, dictates cardiometabolic health, aging, and longevity in ad libitum-fed mice. Cell Metab 19, 418–430, doi:10.1016/j.cmet.2014.02.009 (2014). [PubMed: 24606899]
9. Fontana L et al. Decreased Consumption of Branched-Chain Amino Acids Improves Metabolic Health. Cell reports 16, 520–530, doi:10.1016/j.celrep.2016.05.092 (2016). [PubMed: 27346343]
10. Grandison RC, Piper MD & Partridge L Amino-acid imbalance explains extension of lifespan by dietary restriction in Drosophila. Nature 462, 1061–1064, doi:10.1038/nature08619 (2009). [PubMed: 19956092]
11. Lu J et al. Sestrin is a key regulator of stem cell function and lifespan in response to dietary amino acids. Nature Aging 1, 60–72, doi:10.1038/s43587-020-00001-7 (2021).
12. Solon-Biet SM et al. Branched chain amino acids impact health and lifespan indirectly via amino acid balance and appetite control. Nat Metab 1, 532–545, doi:10.1038/s42255-019-0059-2 (2019). [PubMed: 31656947]
13. Yoshida S et al. Role of dietary amino acid balance in diet restriction-mediated lifespan extension, renoprotection, and muscle weakness in aged mice. Aging Cell 17, e12796, doi:10.1111/acel.12796 (2018). [PubMed: 29943496]
14. Speakman JR, Mitchell SE & Mazidi M Calories or protein? The effect of dietary restriction on lifespan in rodents is explained by calories alone. Exp Gerontol 86, 28–38, doi:10.1016/j.exger.2016.03.011 (2016). [PubMed: 27006163]
15. Acosta-Rodriguez VA, de Groot MHM, Rijo-Ferreira F, Green CB & Takahashi JS Mice under Caloric Restriction Self-Impose a Temporal Restriction of Food Intake as Revealed by an Automated Feeder System. Cell Metab 26, 267–277 e262, doi:10.1016/j.cmet.2017.06.007 (2017). [PubMed: 28683292]

16. Bruss MD, Khambatta CF, Ruby MA, Aggarwal I & Hellerstein MK Calorie restriction increases fatty acid synthesis and whole body fat oxidation rates. Am J Physiol Endocrinol Metab 298, E108–116, doi:10.1152/ajpendo.00524.2009 (2010). [PubMed: 19887594]
17. Longo VD & Mattson MP Fasting: molecular mechanisms and clinical applications. Cell Metab 19, 181–192, doi:10.1016/j.cmet.2013.12.008 (2014). [PubMed: 24440038]
18. Hatori M et al. Time-restricted feeding without reducing caloric intake prevents metabolic diseases in mice fed a high-fat diet. Cell Metab 15, 848–860, doi:10.1016/j.cmet.2012.04.019 (2012). [PubMed: 22608008]
19. Chaix A, Zarrinpar A, Miu P & Panda S Time-restricted feeding is a preventative and therapeutic intervention against diverse nutritional challenges. Cell Metab 20, 991–1005, doi:10.1016/j.cmet.2014.11.001 (2014). [PubMed: 25470547]
20. Mitchell SJ et al. Daily Fasting Improves Health and Survival in Male Mice Independent of Diet Composition and Calories. Cell Metab 29, 221–228 e223, doi:10.1016/j.cmet.2018.08.011 (2019). [PubMed: 30197301]
21. Mitchell SJ et al. Effects of Sex, Strain, and Energy Intake on Hallmarks of Aging in Mice. Cell Metab 23, 1093–1112, doi:10.1016/j.cmet.2016.05.027 (2016). [PubMed: 27304509]
22. Liao CY, Rikke BA, Johnson TE, Diaz V & Nelson JF Genetic variation in the murine lifespan response to dietary restriction: from life extension to life shortening. Aging Cell 9, 92–95, doi:10.1111/j.1474-9726.2009.00533.x (2010). [PubMed: 19878144]
23. Turturro A et al. Growth curves and survival characteristics of the animals used in the Biomarkers of Aging Program. J Gerontol A Biol Sci Med Sci 54, B492–501, doi:10.1093/gerona/54.11.b492 (1999). [PubMed: 10619312]
24. Nelson W & Halberg F Meal-timing, circadian rhythms and life span of mice. The Journal of nutrition 116, 2244–2253, doi:10.1093/jn/116.11.2244 (1986). [PubMed: 3794831]
25. Fernandes G, Yunis EJ & Good RA Influence of diet on survival of mice. Proc Natl Acad Sci U S A 73, 1279–1283, doi:10.1073/pnas.73.4.1279 (1976). [PubMed: 1063408]
26. Hempenstall S, Picchio L, Mitchell SE, Speakman JR & Selman C The impact of acute caloric restriction on the metabolic phenotype in male C57BL/6 and DBA/2 mice. Mech Ageing Dev 131, 111–118, doi:10.1016/j.mad.2009.12.008 (2010). [PubMed: 20064544]
27. Hasek BE et al. Dietary methionine restriction enhances metabolic flexibility and increases uncoupled respiration in both fed and fasted states. Am J Physiol Regul Integr Comp Physiol 299, R728–739, doi:10.1152/ajpregu.00837.2009 (2010). [PubMed: 20538896]
28. Abreu-Vieira G, Xiao C, Gavrilova O & Reitman ML Integration of body temperature into the analysis of energy expenditure in the mouse. Molecular metabolism 4, 461–470, doi:10.1016/j.molmet.2015.03.001 (2015). [PubMed: 26042200]
29. Haws SA, Leech CM & Denu JM Metabolism and the Epigenome: A Dynamic Relationship. Trends Biochem Sci, doi:10.1016/j.tibs.2020.04.002 (2020).
30. Haws SA et al. Methyl-Metabolite Depletion Elicits Adaptive Responses to Support Heterochromatin Stability and Epigenetic Persistence. Mol Cell 78, 210–223 e218, doi:10.1016/j.molcel.2020.03.004 (2020). [PubMed: 32208170]
31. Leatham-Jensen M et al. Lysine 27 of replication-independent histone H3.3 is required for Polycomb target gene silencing but not for gene activation. PLoS Genet 15, e1007932, doi:10.1371/journal.pgen.1007932 (2019). [PubMed: 30699116]
32. Meyer C, Dostou JM, Welle SL & Gerich JE Role of human liver, kidney, and skeletal muscle in postprandial glucose homeostasis. Am J Physiol Endocrinol Metab 282, E419–427, doi:10.1152/ajpendo.00032.2001 (2002). [PubMed: 11788375]
33. Wolfe RR The underappreciated role of muscle in health and disease. Am J Clin Nutr 84, 475–482, doi:10.1093/ajcn/84.3.475 (2006). [PubMed: 16960159]
34. Rhoads TW et al. Molecular and Functional Networks Linked to Sarcopenia Prevention by Caloric Restriction in Rhesus Monkeys. Cell Syst 10, 156–168 e155, doi:10.1016/j.cels.2019.12.002 (2020). [PubMed: 31982367]
35. McKiernan SH et al. Caloric restriction delays aging-induced cellular phenotypes in rhesus monkey skeletal muscle. Exp Gerontol 46, 23–29, doi:10.1016/j.exger.2010.09.011 (2011). [PubMed: 20883771]

36. Pugh TD et al. A shift in energy metabolism anticipates the onset of sarcopenia in rhesus monkeys. Aging Cell 12, 672–681, doi:10.1111/acel.12091 (2013). [PubMed: 23607901]
37. Chang J et al. Effect of aging and caloric restriction on the mitochondrial proteome. J Gerontol A Biol Sci Med Sci 62, 223–234, doi:10.1093/gerona/62.3.223 (2007). [PubMed: 17389719]
38. Parks BW et al. Genetic architecture of insulin resistance in the mouse. Cell Metab 21, 334–347, doi:10.1016/j.cmet.2015.01.002 (2015). [PubMed: 25651185]
39. Xia J, Benner MJ & Hancock RE NetworkAnalyst--integrative approaches for protein-protein interaction network analysis and visual exploration. Nucleic Acids Res 42, W167–174, doi:10.1093/nar/gku443 (2014). [PubMed: 24861621]
40. Xia J et al. INMEX--a web-based tool for integrative meta-analysis of expression data. Nucleic Acids Res 41, W63–70, doi:10.1093/nar/gkt338 (2013). [PubMed: 23766290]
41. Xia J, Gill EE & Hancock RE NetworkAnalyst for statistical, visual and network-based meta-analysis of gene expression data. Nat Protoc 10, 823–844, doi:10.1038/nprot.2015.052 (2015). [PubMed: 25950236]
42. Xia J, Lyle NH, Mayer ML, Pena OM & Hancock RE INVEX--a web-based tool for integrative visualization of expression data. Bioinformatics 29, 3232–3234, doi:10.1093/bioinformatics/btt562 (2013). [PubMed: 24078684]
43. Zhou G et al. NetworkAnalyst 3.0: a visual analytics platform for comprehensive gene expression profiling and meta-analysis. Nucleic Acids Res 47, W234–W241, doi:10.1093/nar/gkz240 (2019). [PubMed: 30931480]
44. Kane AE et al. Impact of Longevity Interventions on a Validated Mouse Clinical Frailty Index. J Gerontol A Biol Sci Med Sci 71, 333–339, doi:10.1093/gerona/glu315 (2016). [PubMed: 25711530]
45. Bellantuono I et al. A toolbox for the longitudinal assessment of healthspan in aging mice. Nature protocols 15, 540–574, doi:10.1038/s41596-019-0256-1 (2020). [PubMed: 31915391]
46. Aon MA et al. Untangling Determinants of Enhanced Health and Lifespan through a Multi-omics Approach in Mice. Cell Metab 32, 100–116 e104, doi:10.1016/j.cmet.2020.04.018 (2020). [PubMed: 32413334]
47. Duffy PH et al. Effect of chronic caloric restriction on physiological variables related to energy metabolism in the male Fischer 344 rat. Mech Ageing Dev 48, 117–133, doi:10.1016/0047-6374(89)90044-4 (1989). [PubMed: 2661930]
48. Masoro EJ, McCarter RJ, Katz MS & McMahan CA Dietary restriction alters characteristics of glucose fuel use. J Gerontol 47, B202–208, doi:10.1093/geronj/47.6.b202 (1992). [PubMed: 1430849]
49. Green CL et al. The effects of graded levels of calorie restriction: IX. Global metabolomic screen reveals modulation of carnitines, sphingolipids and bile acids in the liver of C57BL/6 mice. Aging Cell 16, 529–540, doi:10.1111/acel.12570 (2017). [PubMed: 28139067]
50. Green CL et al. The Effects of Graded Levels of Calorie Restriction: XIV. Global Metabolomics Screen Reveals Brown Adipose Tissue Changes in Amino Acids, Catecholamines, and Antioxidants After Short-Term Restriction in C57BL/6 Mice. J Gerontol A Biol Sci Med Sci 75, 218–229, doi:10.1093/gerona/glz023 (2020). [PubMed: 31220223]
51. Green CL et al. The Effects of Graded Levels of Calorie Restriction: XIII. Global Metabolomics Screen Reveals Graded Changes in Circulating Amino Acids, Vitamins, and Bile Acids in the Plasma of C57BL/6 Mice. J Gerontol A Biol Sci Med Sci 74, 16–26, doi:10.1093/gerona/gly058 (2019). [PubMed: 29718123]
52. Green CL et al. The Effects of Graded Levels of Calorie Restriction: XVI. Metabolomic Changes in the Cerebellum Indicate Activation of Hypothalamocerebellar Connections Driven by Hunger Responses. J Gerontol A Biol Sci Med Sci 76, 601–610, doi:10.1093/gerona/glaa261 (2021). [PubMed: 33053185]
53. Kokkonen GC & Barrows CH The effect of dietary cellulose on life span and biochemical variables of male mice. Age 11, 7–9, doi:10.1007/BF02431758 (1988).
54. Mair W, Piper MD & Partridge L Calories do not explain extension of life span by dietary restriction in Drosophila. PLoS Biol 3, e223, doi:10.1371/journal.pbio.0030223 (2005). [PubMed: 16000018]

55. Greer EL & Brunet A Different dietary restriction regimens extend lifespan by both independent and overlapping genetic pathways in C. elegans. Aging Cell 8, 113–127, doi:10.1111/j.1474-9726.2009.00459.x (2009). [PubMed: 19239417]
56. Lyn JC, Naikkhwah W, Aksenov V & Rollo CD Influence of two methods of dietary restriction on life history features and aging of the cricket Acheta domesticus. Age (Dordr) 33, 509–522, doi:10.1007/s11357-010-9195-z (2011). [PubMed: 21120631]
57. Derous D et al. The Effects of Graded Levels of Calorie Restriction: X. Transcriptomic Responses of Epididymal Adipose Tissue. The Journals of Gerontology: Series A 73, 279–288, doi:10.1093/gerona/glx101 (2017).
58. Derous D et al. The effects of graded levels of calorie restriction: XI. Evaluation of the main hypotheses underpinning the life extension effects of CR using the hepatic transcriptome. Aging (Albany NY) 9, 1770–1824, doi:10.18632/aging.101269 (2017). [PubMed: 28768896]
59. Froy O & Miskin R Effect of feeding regimens on circadian rhythms: implications for aging and longevity. Aging (Albany NY) 2, 7–27, doi:10.18632/aging.100116 (2010). [PubMed: 20228939]
60. Barrington WT et al. Improving Metabolic Health Through Precision Dietetics in Mice. Genetics 208, 399–417, doi:10.1534/genetics.117.300536 (2018). [PubMed: 29158425]
61. Chaix A, Lin T, Le HD, Chang MW & Panda S Time-Restricted Feeding Prevents Obesity and Metabolic Syndrome in Mice Lacking a Circadian Clock. Cell Metab 29, 303–319 e304, doi:10.1016/j.cmet.2018.08.004 (2019). [PubMed: 30174302]
62. Sutton EF et al. Early Time-Restricted Feeding Improves Insulin Sensitivity, Blood Pressure, and Oxidative Stress Even without Weight Loss in Men with Prediabetes. Cell Metab 27, 1212–1221 e1213, doi:10.1016/j.cmet.2018.04.010 (2018). [PubMed: 29754952]
63. Colman RJ et al. Caloric restriction delays disease onset and mortality in rhesus monkeys. Science 325, 201–204, doi:10.1126/science.1173635 (2009). [PubMed: 19590001]
64. Mattison JA et al. Impact of caloric restriction on health and survival in rhesus monkeys from the NIA study. Nature 489, 318–321, doi:10.1038/nature11432 (2012). [PubMed: 22932268]
65. Mattison JA et al. Caloric restriction improves health and survival of rhesus monkeys. Nature communications 8, 14063, doi:10.1038/ncomms14063 (2017).
66. Ramsey JJ et al. Dietary restriction and aging in rhesus monkeys: the University of Wisconsin study. Exp Gerontol 35, 1131–1149, doi:10.1016/s0531-5565(00)00166-2 (2000). [PubMed: 11113597]
67. Cienfuegos S et al. Effects of 4- and 6-h Time-Restricted Feeding on Weight and Cardiometabolic Health: A Randomized Controlled Trial in Adults with Obesity. Cell Metab 32, 366–378 e363, doi:10.1016/j.cmet.2020.06.018 (2020). [PubMed: 32673591]
68. Wilkinson MJ et al. Ten-Hour Time-Restricted Eating Reduces Weight, Blood Pressure, and Atherogenic Lipids in Patients with Metabolic Syndrome. Cell Metab 31, 92–104 e105, doi:10.1016/j.cmet.2019.11.004 (2020). [PubMed: 31813824]
69. Yokoyama Y et al. Erratum for Yokoyama et al., "Skipping Breakfast and Risk of Mortality from Cancer, Circulatory Diseases and All Causes: Findings from the Japan Collaborative Cohort Study". Yonago Acta Med 62, 308, doi:10.33160/yam.2019.11.007 (2019). [PubMed: 31915412]
70. Uzhova I et al. The Importance of Breakfast in Atherosclerosis Disease: Insights From the PESA Study. Journal of the American College of Cardiology 70, 1833–1842, doi:10.1016/j.jacc.2017.08.027 (2017). [PubMed: 28982495]
71. Cornelissen G When You Eat Matters: 60 Years of Franz Halberg's Nutrition Chronomics. The Open Nutraceuticals Journal 5, 16–44, doi:10.2174/1876396001205010016 (2012).
72. Stote KS et al. A controlled trial of reduced meal frequency without caloric restriction in healthy, normal-weight, middle-aged adults. Am J Clin Nutr 85, 981–988, doi:10.1093/ajcn/85.4.981 (2007). [PubMed: 17413096]
73. Carlson O et al. Impact of reduced meal frequency without caloric restriction on glucose regulation in healthy, normal-weight middle-aged men and women. Metabolism 56, 1729–1734, doi:10.1016/j.metabol.2007.07.018 (2007). [PubMed: 17998028]
74. Arnason TG, Bowen MW & Mansell KD Effects of intermittent fasting on health markers in those with type 2 diabetes: A pilot study. World J Diabetes 8, 154–164, doi:10.4239/wjd.v8.i4.154 (2017). [PubMed: 28465792]

75. Dommerholt MB, Dionne DA, Hutchinson DF, Kruit JK & Johnson JD Metabolic effects of short-term caloric restriction in mice with reduced insulin gene dosage. J Endocrinol 237, 59–71, doi:10.1530/JOE-17-0505 (2018). [PubMed: 29439088]

76. Melamud E, Vastag L & Rabinowitz JD Metabolomic analysis and visualization engine for LC-MS data. Anal Chem 82, 9818–9826, doi:10.1021/ac1021166 (2010). [PubMed: 21049934]

77. Clasquin MF, Melamud E & Rabinowitz JD LC-MS data processing with MAVEN: a metabolomic analysis and visualization engine. Curr Protoc Bioinformatics Chapter 14, Unit14 11, doi:10.1002/0471250953.bi1411s37 (2012).

78. Whitehead JC et al. A clinical frailty index in aging mice: comparisons with frailty index data in humans. J Gerontol A Biol Sci Med Sci 69, 621–632, doi:10.1093/gerona/glt136 (2014). [PubMed: 24051346]

79. Liang H et al. Genetic mouse models of extended lifespan. Exp Gerontol 38, 1353–1364 (2003). [PubMed: 14698816]

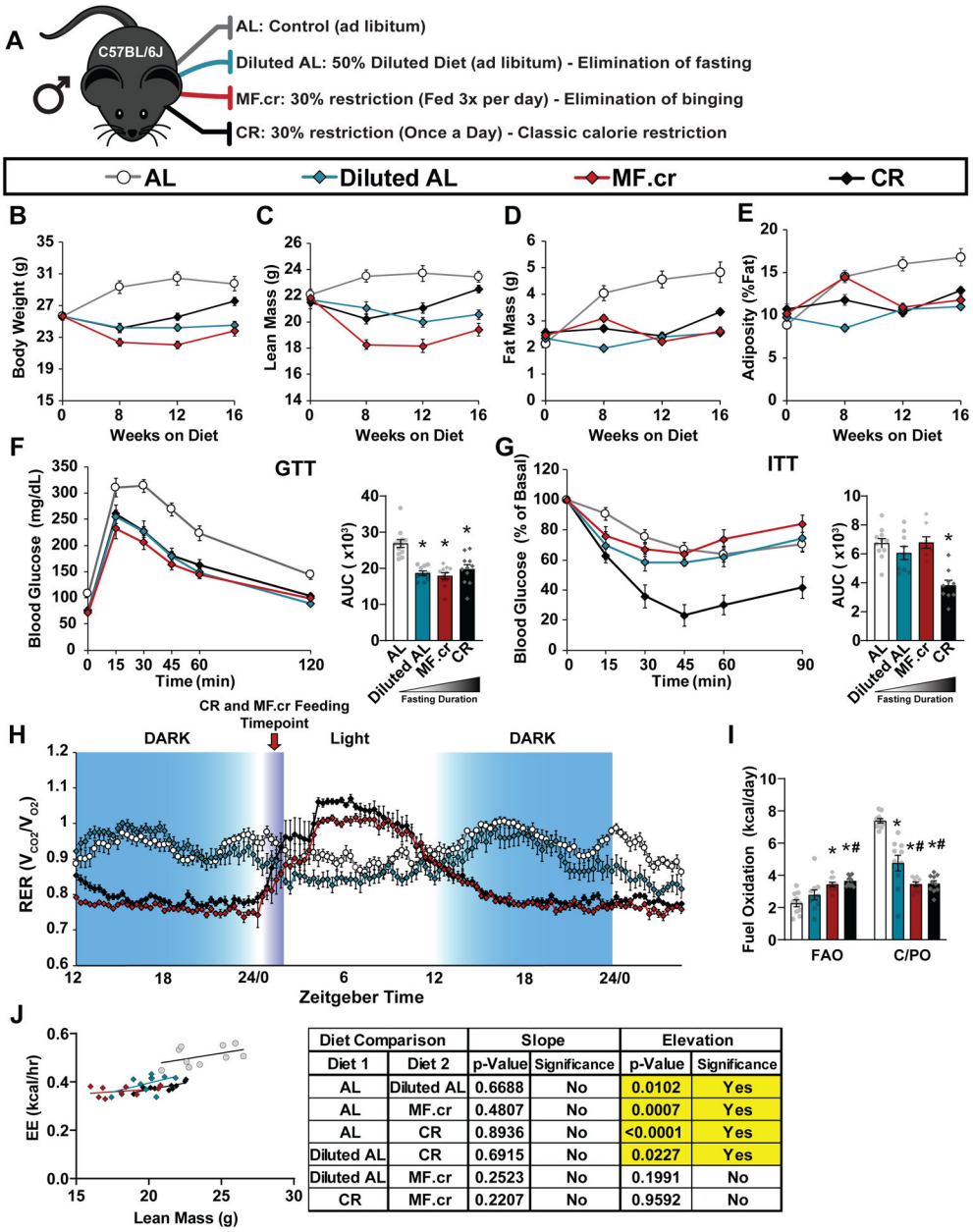

Diet Comparison		Slope		Elevation	
Diet 1	Diet 2	p-Value	Significance	p-Value	Significance
AL	Diluted AL	0.6688	No	0.0102	Yes
AL	MF.cr	0.4807	No	0.0007	Yes
AL	CR	0.8936	No	<0.0001	Yes
Diluted AL	CR	0.6915	No	0.0227	Yes
Diluted AL	MF.cr	0.2523	No	0.1991	No
CR	MF.cr	0.2207	No	0.9592	No

Figure 1: Prolonged fasting is required for the CR-mediated increase in insulin sensitivity and alterations in fuel source selection in male C57BL/6J mice.

(A) Outline of feeding regimens: AL, Diluted AL, CR and MF.cr. (B-E) Body composition measurement over 16 weeks on diet (n = 10 biologically independent mice per diet); total body weight (B), lean mass (C), fat mass (D) and adiposity (E). (F-G) Glucose (AL, n = 12; Diluted AL, n = 10; MF.cr, n = 11; CR, n = 11 biologically independent mice) (F) and insulin (AL, n = 11; Diluted AL, n = 9; MF.cr, n = 8; CR, n = 9 biologically independent mice) (G) tolerance tests after 9 or 10 weeks on the indicated diets. * symbol represents a significant difference versus AL-fed mice (P<0.0001) based on Tukey's test post one-way ANOVA. (H-J) Metabolic chamber analysis of mice fed the indicated diets. (H) Respiratory exchange ratio vs. time (n = 10 biologically independent mice per diet) (I) Fuel utilization

was calculated for the 24-hour period following the indicated (arrow) refeeding time (n = 10 biologically independent mice per diet). ***** symbol represents a significant difference versus AL (Diluted AL, $p < 0.0001$; MF.cr, $p \leq 0.0018$; CR, $p \leq 0.0002$); # symbol represents a significant difference versus Diluted AL (MF.cr, $p = 0.0097$; CR, $p \leq 0.0283$) based on Tukey's test post one-way ANOVA performed separately for FAO and C/PO). (J) Energy expenditure as a function of lean mass was calculated for the 24-hour period following the indicated (arrow) refeeding time (n = 10 mice per diet, data for each individual mouse is plotted; slopes and intercepts were calculated using ANCOVA). All data are represented as mean ± SEM.

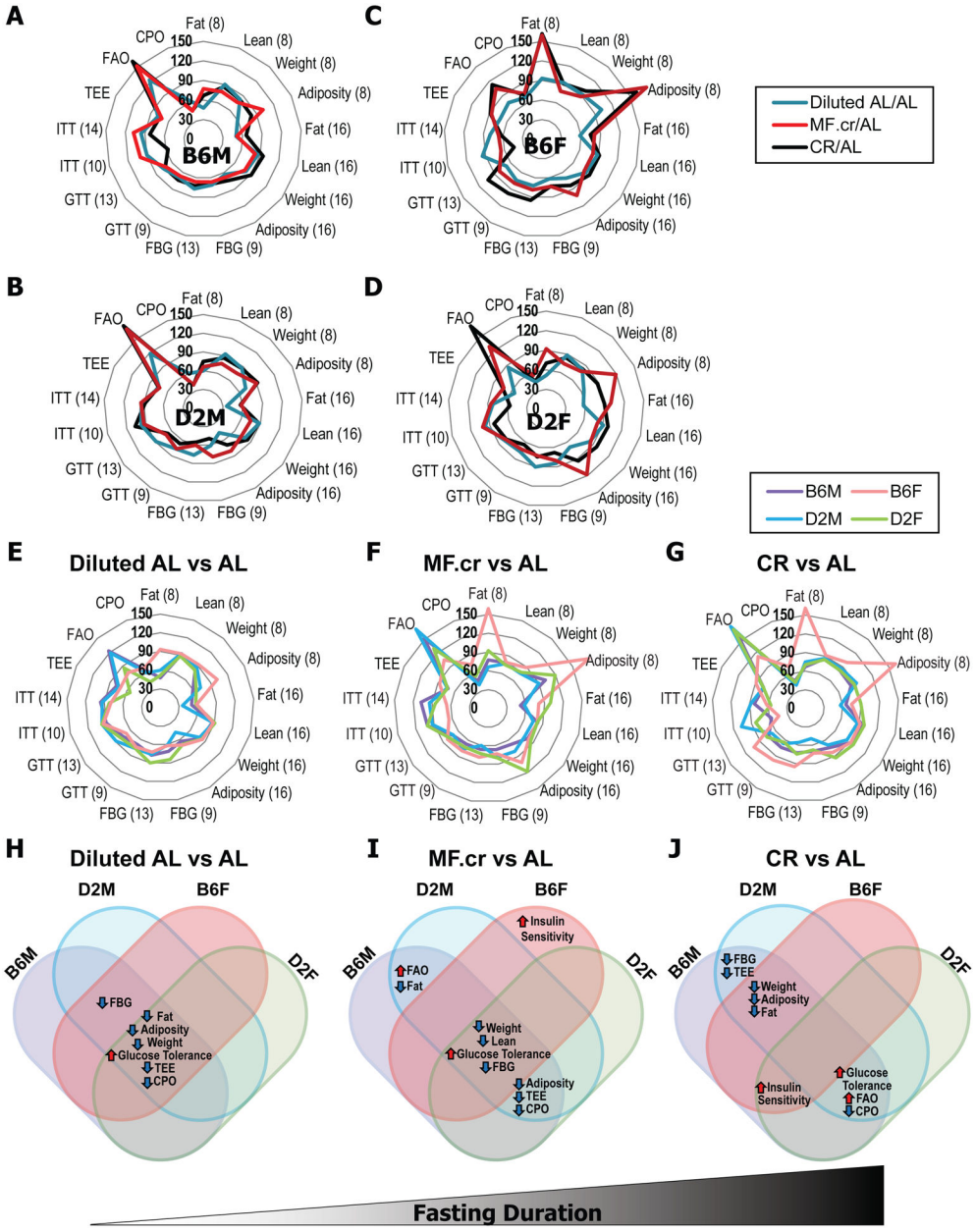

Figure 2: Distinct physiological responses to diet in different strains and sexes of mice.

(A-G) Radar chart visualization of 17 phenotypes measured in C57BL/6J and DBA/2J male and female mice while consuming the indicated diets. (A-D) The distance from the center represents the effect of each restricted diet vs. AL-fed mice (no difference = 100%; Blue – Diluted AL; Red – MF.cr; Black – CR). (E-G) The distance from the center represents the effect of (E) Diluted AL-fed vs. AL, (F) MF.cr-fed vs. AL-fed, and (G) CR vs. AL for the indicated strain and sexes of mice (no difference = 100%). FBG = Fasting blood glucose, GTT and ITT = computed area under the curve for each test; number in parentheses refers to the weeks on the diet each phenotype was determined. (H-J) Summary comparison of diet effect on phenotypes compared to AL for each strain and sex.

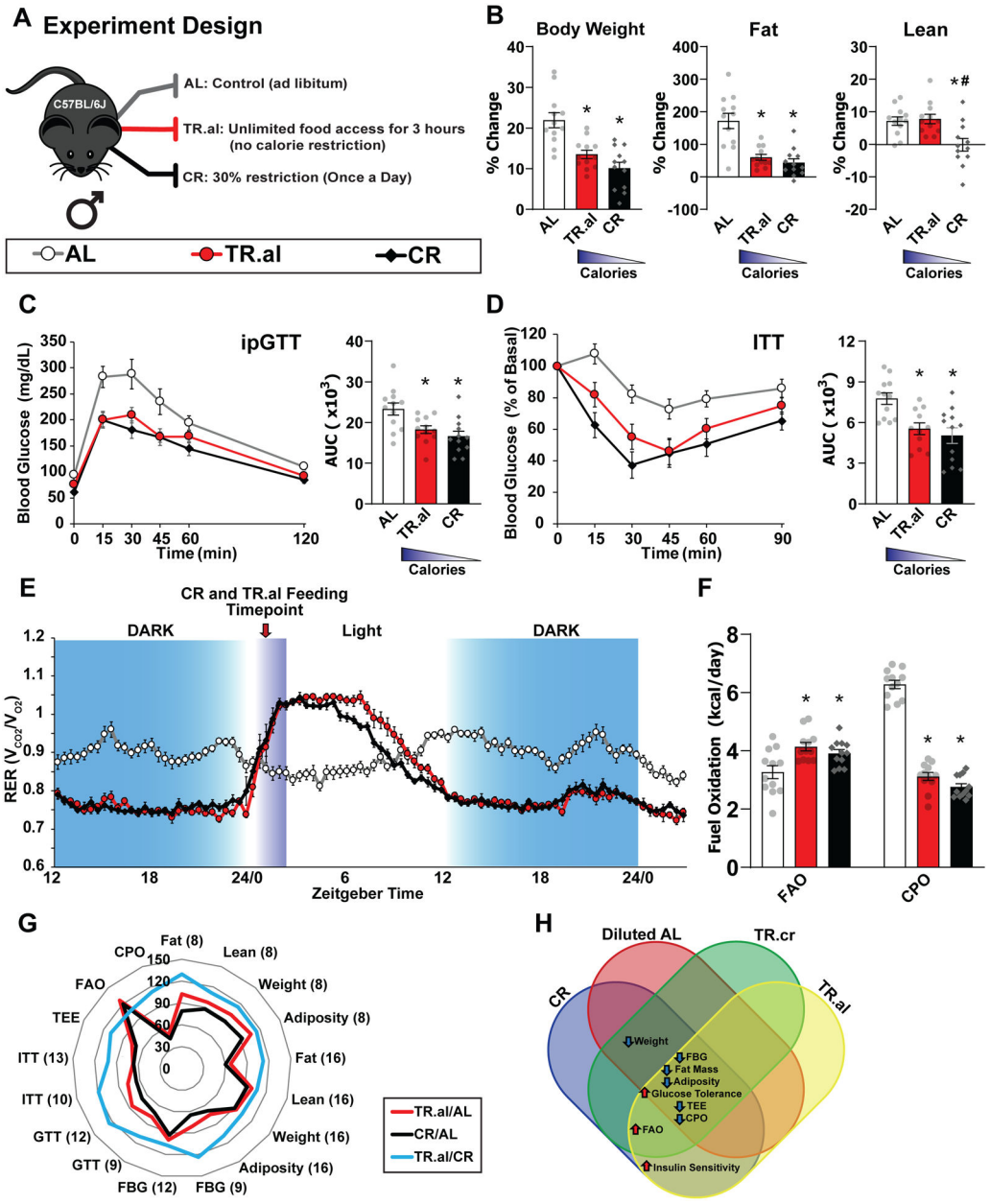

Figure 3: Fasting alone recapitulates the metabolic effects of a CR diet.

A) Schematic of feeding paradigms: AL, TR.al, and CR. B) Change in body weight, fat, and lean mass over the course of 16 weeks consuming the indicated diets (n = 12 biologically independent mice per diet). (C-D) Glucose (n = 12 biologically independent mice per diet) * symbol represents a significant difference versus AL-fed mice (TR.al, p = 0.0204; CR, p = 0.0019) based on Tukey's test post one-way ANOVA. (C) and insulin (AL, n = 12; TR.al, n = 11; n = 8; CR, n = 12 biologically independent mice) * symbol represents a significant difference versus AL-fed mice (TR.al, p = 0.0086; CR, p = 0.0010) based on Tukey's test post one-way ANOVA. (D) tolerance tests were conducted after mice were fed the indicated diets for 9 or 10 weeks, respectively. E) Respiratory exchange ratio (RER) vs. time (n = 12 biologically independent mice per diet). F) Fuel utilization was calculated for the 24-hour

period following the indicated (arrow) refeeding time (n = 12 biologically independent mice per diet). ***** symbol represents a significant difference versus AL (TR.al, $p \leq 0.0027$; CR, $p \leq 0.0306$) based on Tukey's test post one-way ANOVA performed separately for FAO and C/PO). G) Radar chart visualization of 17 phenotypes measured in male C57BL/6J while consuming the indicated diets. (A-G) H) Comparison of diet effect on the phenotypes of C57BL/6J male mice for all feeding regimens examined in this manuscript. All data are represented as mean ± SEM.

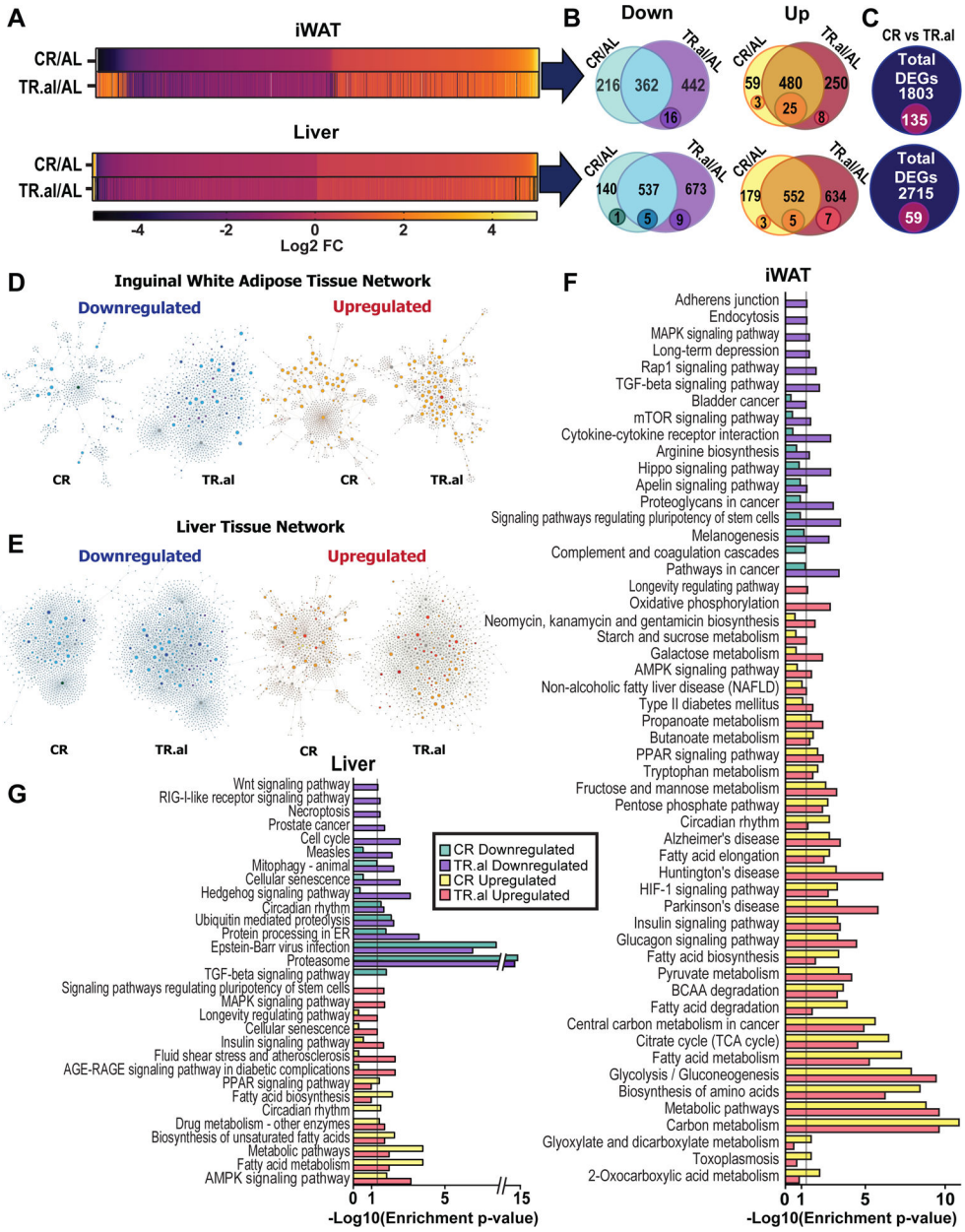

Figure 4: Fasting and calorie restriction result in highly similar transcriptomic signatures in liver and white adipose tissue.

Transcriptional profiling was performed on liver and iWAT from mice fed the AL, CR, or TR.al regimens (n = 6 per diet group). (A) Heatmap of differently expressed genes of CR and TR.al-fed mice compared to AL-fed mice in liver and iWAT. (B-C) Overlap between genes differentially expressed in CR-fed mice and TR.al-fed mice relative to AL-fed mice. Numbers in Venn diagrams represent the number of genes (large circle) and functionally enriched pathways (small circle) identified found from network construction in D-E. (D-E) Network construction of significantly upregulated and downregulated genes of CR and TR.al group in iWAT (D) and liver (E) using NetworkAnalyst. Node size represents number of edges connected to a node and the colors represented by directionality of enrichment.

Downregulated: green – CR specific, light blue – CR and TR.al $p<0.05$, dark blue – CR and TR.al with only TR.al $p<0.05$, purple – TR.al specific $p<0.05$, gray – edges and unknown nodes. Upregulated: yellow – CR specific, orange – CR and TR.al $p<0.05$, dark orange – CR and TR.al with only TR.al $p<0.05$, red – TR.al specific $p<0.05$, gray – edges and unknown nodes. (F-G) Significantly upregulated and downregulated pathways identified from network construction in iWAT (F) and liver (G). Bar graphs represents pathways identified enriched in CR and/or TR.al-fed mice with enrichment $p<0.05$ as computed with the hypergeometric test.

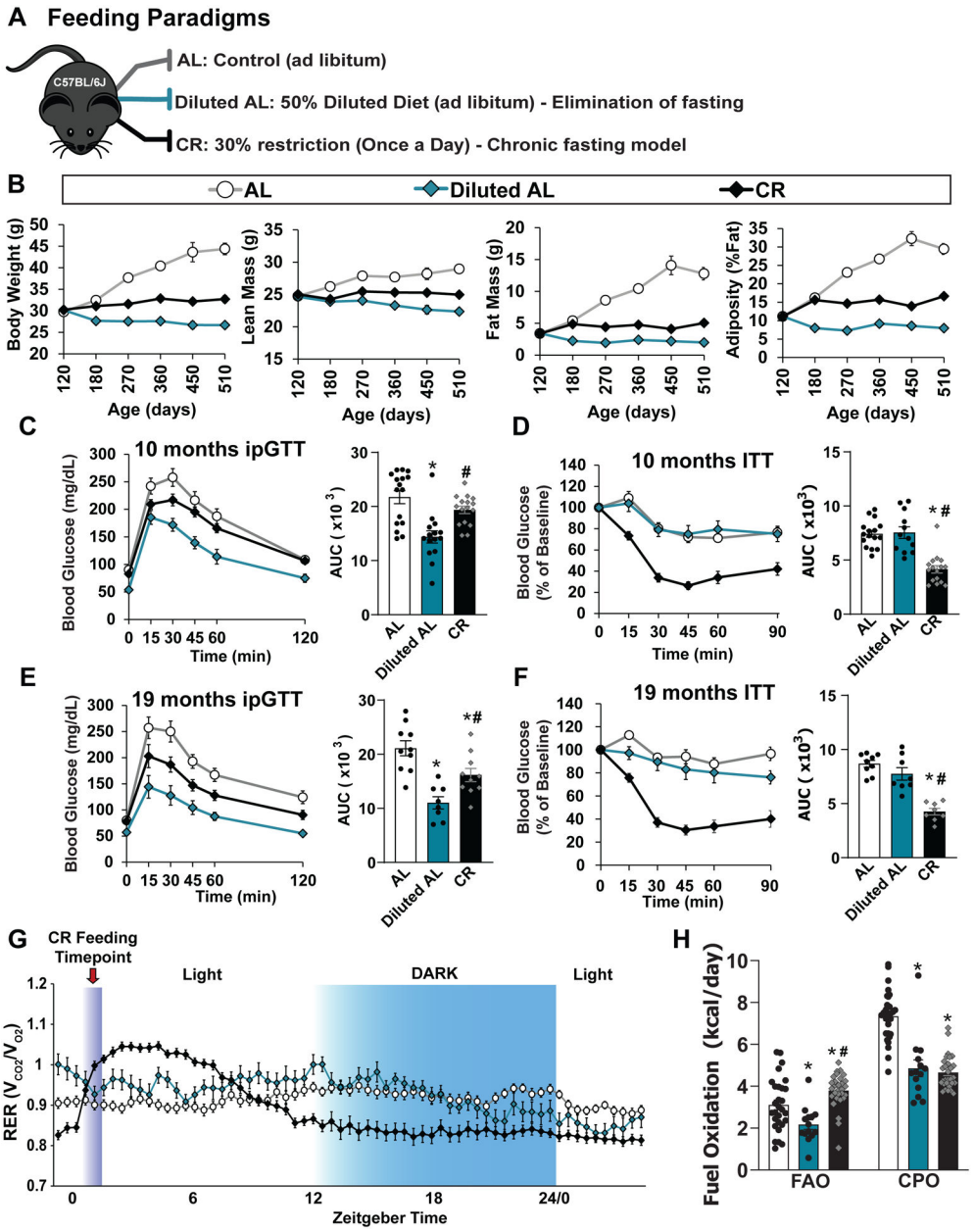

Figure 5. Prolonged fasting is required for the CR-mediated increase in insulin sensitivity and fuel selection in aged mice.

(A) Outline of feeding paradigms: AL, Diluted AL and CR. Diets were fed to C57BL/6J male mice starting at 4 months of age. (B) Change in body composition (body weight, fat mass, lean mass and adiposity) were tracked longitudinally (n varies by days; AL, n= 12–33; Diluted AL, n = 13–33 mice; CR, n = 13–33 biologically independent mice; statistics in Supplementary Table 10). (C) Glucose tolerance test performed at 10 months of age (AL, n = 16; Diluted AL, n = 15; CR, n = 16 biologically independent mice). ***** symbol represents a significant difference versus AL-fed mice (Diluted AL, $p < 0.0001$); # symbol represents a significant difference versus Diluted AL-fed mice (CR, $p = 0.0040$) based on Tukey's test post one-way ANOVA. (D) Insulin tolerance test performed at 10 months

of age (AL, n = 16; Diluted AL, n = 12; CR, n = 16 biologically independent mice). ***** symbol represents a significant difference versus AL-fed mice (CR, $p < 0.0001$); # symbol represents a significant difference versus Diluted AL-fed mice (CR, $p<0.0001$) based on Tukey's test post one-way ANOVA. (E) Glucose tolerance test performed at 19 months of age (AL, n = 10; Diluted AL, n = 8; CR, n = 10 biologically independent mice). ***** symbol represents a significant difference versus AL-fed mice (Diluted AL, $p <0.0001$; CR, $p = 0.0237$); # symbol represents a significant difference versus Diluted AL-fed mice (CR, $p = 0.0270$) based on Tukey's test post one-way ANOVA. F) Insulin tolerance test performed at 19 months of age (AL, n = 9; Diluted AL, n = 8; CR, n = 8 biologically independent mice). ***** symbol represents a significant difference versus AL-fed mice (CR, $p < 0.0001$); # symbol represents a significant difference versus Diluted AL-fed mice (CR, $p < 0.0001$) based on Tukey's test post one-way ANOVA. (G) Respiratory exchange ratio vs. time at ~15 months in age (AL, n = 29; Diluted AL, n = 13; CR, n = 29 biologically independent mice). (H) Fuel utilization was calculated for the 24-hour period following the indicated (arrow) refeeding time (AL, n = 29; Diluted AL, n = 13; CR, n = 29 biologically independent mice). ***** symbol represents a significant difference versus AL (Diluted AL, $p = 0.0179$; CR, $p = 0.0352$); # symbol represents a significant difference versus Diluted AL (CR, $p \leq 0.0001$) based on Tukey's test post one-way ANOVA performed separately for FAO and C/PO). All data are represented as mean ± SEM.

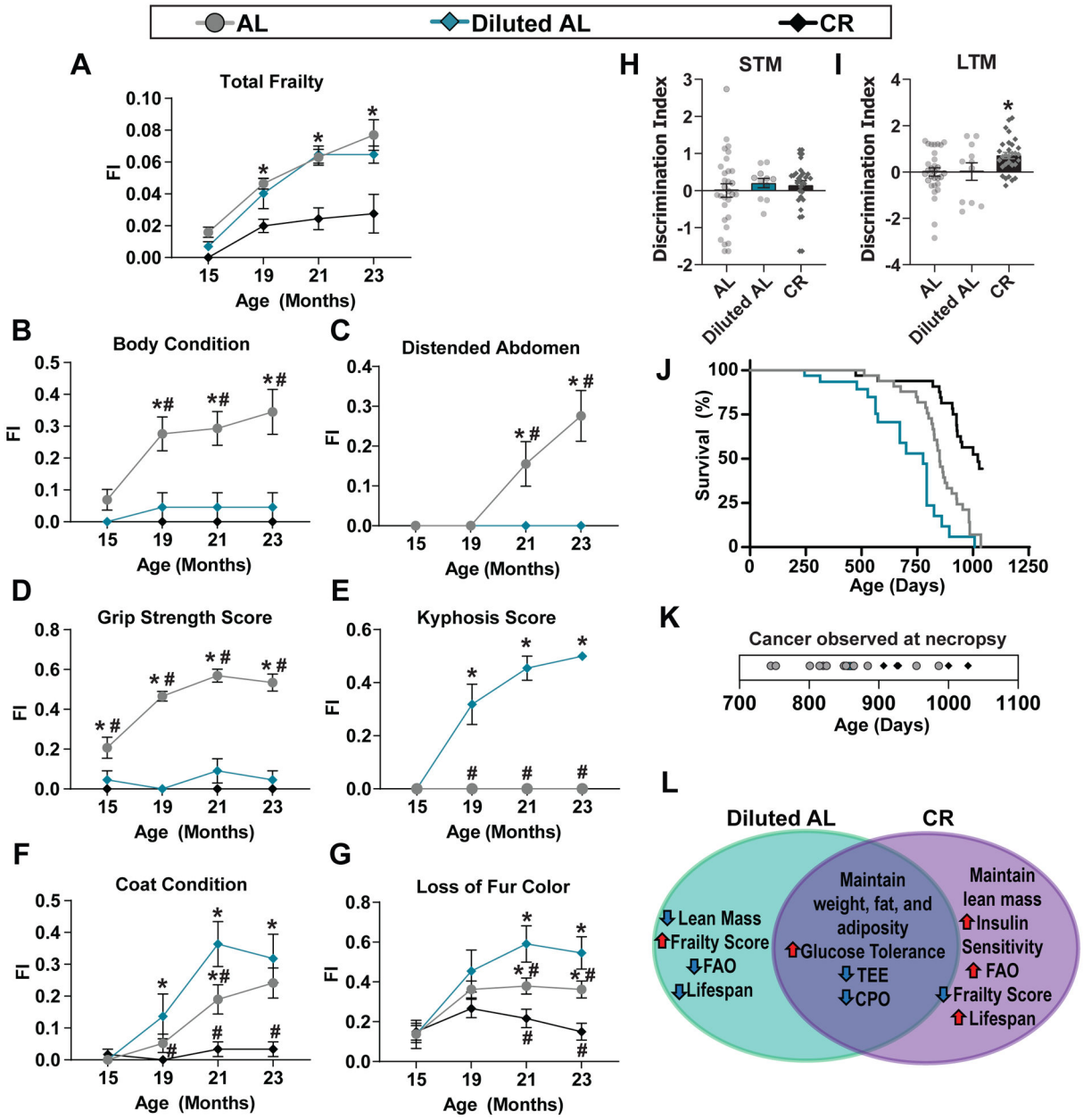

Figure 6. Fasting is required for the geroprotective effects of a CR diet.

(A-G) Frailty of mice was determined from 15–23 months of age and mice that did not survive up to 23 months of age were excluded. Total Frailty (A); specific deficits (B-G) of interests scored as part of the clinical frailty index. (A-G) AL; n = 29, Diluted AL, n = 11, CR, n = 30 biologically independent mice; * symbol represents a significant difference versus AL (CR, $p < 0.0001$); # symbol represents a significant difference versus Diluted AL (CR, $p < 0.0001$), based on Tukey's test post two-way ANOVA. (H-I) A novel object recognition test was performed at 21 months of age to assess (H) short-term (STM) and (I) long-term (LTM) memory. AL; n = 30, Diluted AL, n = 11, CR, n = 30 biologically independent mice; * symbol represents a significant difference versus AL (CR, $p < 0.0001$); # symbol represents a significant difference versus Diluted AL (CR, $p < 0.0001$), based on

Tukey's test post two-way ANOVA.(J) Kaplan-Meier plot of the lifespan of mice on the indicated diets starting at 4 months of age; Log-rank test (Mantel-Cox), $p < 0.0001$, AL vs. Diluted AL and AL vs. CR; log-rank test for trend , $p = 0.0001$, AL vs. Diluted AL and AL vs. CR. (K) Tumors observed at the time of necropsy; each dot representing a single mouse. (L) Comparison of phenotypes induced by Diluted AL and CR diets, as compared to AL. All data are represented as mean ± SEM.

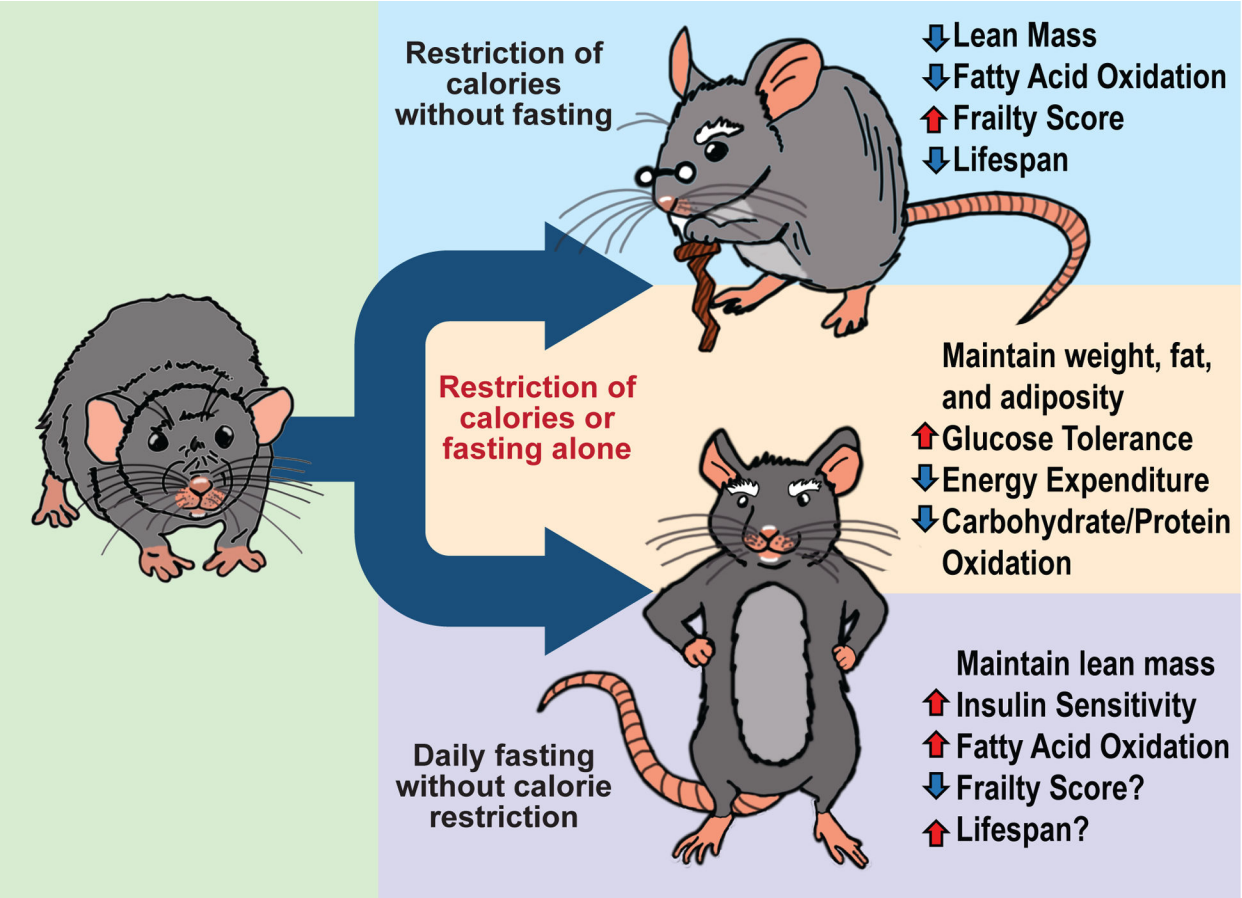

Figure 7.
Fasting plays a critical role in the response to a CR diet.